aa

Joel Luan de Racskai Robert Astudillo

Dissertation to obtain the Master Degree of
Master of Science in
Micro and Nanotechnologies Engineering

Manufacture and viability assessment of a composite Ti/HAp coating for replacement of single HAp layers on stainless steel type 316 medical implant spinal screws

Adviser: Dr.Eduardo Ascenso Pires, CEO, Ceramed .S.A.

Co-adviser: João Paulo Borges, Associated Professor, FCT NOVA

Examination Committee

April, 2019

[Manufacture and viability assessment of a composite Ti/HAp coating for substitute single HAp layers on stainless steel type 316 medical implant spinal screws]

“Man is lazy, in general, to think all that is thinkable, and is content with fragments of ideas, refusing absolute coherence. It does not take the effort to understand to the end. And, precisely because it does not, it takes, in relation to its capacity of intelligence, an absurd position of pride. Compare what little he understood with the least that others understood, never with how much the rarest could perceive.”

Agostinho da Silva

Acknowledgments

This dissertation would not be possible without a very large group of people that accompanied, helped and guided me during this project but also throw out my scholar, academic and personal life.

In order to thank everyone for this opportunity I would like to start with my advisor Dr. Eduardo Ascenso Pires, for receiving me at CERAMED SA. His professional knowhow, guidance and support made this dissertation possible. I would like to dedicate a special thanks to Ana Carina Duarte the General Manager, Lidia Ricardo Quality Responsible and André Baião Quality Control Responsible since it was them that helped me and passed through all the knowledge to perform a vast range and variety of technical procedures, notions and tasks that allowed me to execute this dissertation. Also a special thanks to all the staff in Plasma Spray Production Department, Pedro Moura the Plasma Spray Responsible and Gonçalo Ribeiro Plasma Spray Operator that helped during all these months with their assistance and guidance operating the APS system.

I would like to thank as well to my supervisor at FCT, Professor Dr. João Paulo Borges, for his guidance and overall support on this project. To highlight his overall patience, availability and time dedicated to my dissertation. Would also like to thank all the assistant teachers and staff at FCT campus that helped me during my tasks and analysis, with a special emphasis to Professor. Joana Pinto and researcher Andreia Lopes.

Also a special thanks to Pedro Prazeres from Paralab LDA, for allowing the use of the SEM equipment Phenon PRO-X, since it prove to be very useful.

To my parents Ana Robert and Fernando Raposo, I would not have enough pages to write down all that I am thankful for. But in a short resume I want to thank them their continuous and unconditional support, their forever readiness to help and give me all the right tools to succeed in life. A special thanks to my grandparents Katharina and Victor Robert for they are the people who did look out for the rest of the family, they imbued all the principles and values that we hold dear, and I sincerely hope that I will raise in life to be closer to what they expect me too.

A special thanks to my girlfriend Maria João Sodré, for all her patience and continuous care in every good and bad part of this quest that is life. Could not wish for a better companionship and friend, and I am sure we will have plenty of new challenges to face together in the future.

Last but not least a really big thank you to all my close and longtime friends, they know who they are and know me better than most and what it was too grew until the point where we stand. A long journey full of joys, enrichment and fulfillment and along the way plenty of deviations, bumps and turns. But in the end we still stand together,

closer then never and better persons than before, by that I am sure we took the right way.

A final thanks to the FCT NOVA for allowing me to study in such a prestigious institution, to reach my goals and become an Engineer. Thank you very much!

.

Resumo

Os parafusos paras implantes médicos usados actualmente contam com uma fina camada de Hidroxiapatite para melhorar a fixação da interface implante-osso, porém este revestimento apresenta desempenho com fraca resistência mecânica ao substrato.

Avanços recentes na pesquisa em ciência de materiais exploraram a produção de revestimento compositos para uso na indústria de revestimentos de implantes médicos. Este novo campo de abordagens de engenharia, permitiu uma alternativa promissora mais barata e melhorada comparando com os atuais métodos de produção usando apenas hidroxiapatita. Os interesses da CERAMED SA em desenvolver revestimentos novos e mais baratos através Plasma Spray em ambiente Atmosférico culminaram neste trabalho. Foi produzido por Turbula mixing um compósito misturando por J3 horas a 101 RPM, pós comerciais disponíveis de Titanium e Hidroxiapatite em uso nas instalações durante este estudo com certa granulometria com tamanho de partícula variando entre [5-200] e [15-200] µm respectivamente e densidade de 4,522 e 3,148 g/cm^3 respectivamente. Este pó compósito é utilizado através de um sistema de Spray de Plasma Atmosférico para transformá-lo em um revestimento para uso específico em parafusos de implante de aço inoxidável tipo 316L. Com base na literatura anterior e nos equipamentos e materiais disponíveis nas instalações da CERAMED S.A., foi criado o programa Atmospheric Plasma Spray 1. Para este programa foi feito um estudo usando parâmetros primários pré-selecionados para entender a influência direta dos parâmetros do sistema de pulverização do Plasma Atmosférico, nas propriedades do revestimento como espessura, força de adesão, cristalinidade do revestimento e rugosidade.

O revestimento apresentou bons resultados na resistência à tração em um amplo conjunto de faixas mostrando melhor resistência à adesão em comparação com a hidroxiapatita, no entanto, o cristal-linimento apresentou resultados abaixo do necessário para uso comercial. Utilizando 4 fatores principais do sistema de Pulverização Primária de Plasma (Distância do Noozle, Potência do Plasma, Fluxo de Gás Secundário e Fluxo de Gás Secundário), um Desenho de experiências usandos 2 melhores níveis dentro do intervalo para cada parametro. Utilizando um estudo fatorial completo de experiências, foi realizada uma análise de variância e foi calculado o melhor conjunto de níveis para cada fator. O intervalo de resultados previsto mostrou estar próximo dos requisitos padrão, mas não em conformidade, entre [34,16-39,66]% de cristalinidade. Uma expericia de confirmação foi realizada utilizando para a cristalinidade com um valor de 34,31% e a força de adesão do revestimento apresentou um valor de 18,89 ± 3,76 MPa, consideravelmente acima dos valores para camadas simples de HAp.

.

Abstract

Current medical implant spinal screws rely on a thin Hydroxyapatite layer to improve bone-implant fixation, however this coating presents weak mechanical strength performance.

Recent advances in materials science research have explored the production of composite coating for the use in medical implant coatings industry. This new field of composite engineering approaches, enabled a promising cheaper and improved alternative to current production methods using solely Hydroxyapatite. CERAMED S.A. interest on developing new upgraded and cheaper Atmospheric Plasma Spray coatings culminated on this work where it was manufactured by Turbula mixing a composite powder for J3 at 101 RPM, using known at the time of this study available commercial powders of Titanium and Hydroxyapatite of size range [5-200] and [15-200] µm respectively and density 4,522 and 3,148 g/cm^3 respectively. This composite powder is used trough an Atmospheric Plasma Spray system to transform it into a coating hard coating for specific use in stainless steel type 316 implant spinal screws. Based on previous literature and available equipment and materials at CERAMED S.A. facilities, an Atmospheric Plasma Spray program 1 was created. A preliminary study using, pre-selected primary parameters was made to understand the direct influence of Atmospheric Plasma spray system parameters, on coating properties like thickness, pull-out strength, coating crystallinity and roughness. The coating showed good results on pull out strength on trough a wide set of ranges showing an improved adhesion strength compared to Hydroxyapatite, however crystallinity presented results under the required for commercial usage. Using 4 main primary Plasma Spray system factors (Nozzle Distance, Plasma Power, Primary Gas Flow and Secondary Gas Flow), a Design of experiments using 2 best levels within the range. By using a full factorial study design of experiences an analysis of variance was performed and the best set of levels for each factor was calculated. Predicted range of results showed to be close to standard requirements but not in compliance, between [34,16- 39,66] % of crystallinity. A confirmation experience was performed using the best levels for crystallinity with a value of 34,31% and adhesion strength of the coating showed a value of 18,89 ± 3,76 MPa, considerably above the values for single HAp.

Acronym

Acronym	Meaning
AC	Alternate Current
APS	Atmospheric Plasma Spray
ASTM	American Society for Testing and Materials
DC	Direct Current
HAp	Hydroxyapatite
ISO	International Organization for Standardization
Ti	Titanium
FDA	Federal Drug Agency (USA)
XRD	X- Ray Diffraction
FRX	Fluroscence X-Ray
SEM	Scanning Electron Microscopy

Content

List of Figures

List de Tables

Motivation

The objective of this study was to produce and then to test the viability of a composite coating made of Hydroxyapatite and Titanium in order to evaluate its reliability to replace current simple HAp coatings on stainless steel spinal screws.

Due to their weak mechanical properties porous Hydroxyapatite can only be applied where the mechanical forces are low. Many investigators have developed methods for coating ceramics on top of metals (double/graded) or to create biocomposites coatings, however little research has been done in the use of these in stainless steel spinal screws.

At CERAMED usually for coating medical implant spinal screws, HAp layers always present a thicknesses under 100 µm where the current double Ti and HAp layer coatings are not feasible due to the sheer particle size in the powder used (impossible to achieve such a fin layer using current Titanium range sizes) and graded coatings are incompatible with a complex sHApe such has a spinal screw thread. The goal is to create a composite coating using HAp and Titanium and to evaluate if it is possible to improve the coating performance on needed features such as adhesion strength (pull-out) to the stainless steel substrate, however high crystallinity and overall good looking uniformity are required to become a reliable product.

It is also the objective of the present dissertation to develop such technology using simple methods that can be easily adapted to be used at the company facilities and that are inexpensive and applicable to mass production. This dissertation work aims to:

- Develop a composite easy and cheap to produce;
- Produce a coating that can outperform HAp in terms of adhesion strength (>15 MPa);
- Produce a coating that presents crystallinity higher than 45% according to standard production requirements and the FDA;
- Produce a coating that is not more expensive than the current single HAp layer method;

1 Introduction

1.1 Medical Devices Implants Spinal screws

There are over 5.600.000 people in the United States alone that sustain fractures each year, and many more worldwide. Internal fixation is an operation in orthopedics that involves the surgical implementation of implants for the purpose of repairing a bone, a concept that dates to the mid-nineteenth century and was made applicable for routine treatment in the mid-twentieth century [1]. Internal fixation allows shorter hospital stays, enables patients to return to function earlier, and reduces the incidence of nonunion (improper healing) and malunion (healing in improper position) of broken bones [2].

If a bone is so badly fractured that it will not heal if it is put in a cast, special implants, such as plates, spinal screws, nails and wires [3] are used to pull the pieces of the bone together and to stabilize them before a cast is applied. The primary functional objective in the design of a spinal screw is to dissipate and distribute the mechanical load. For this objective thread design should maximize initial contact, enhance surface area, dissipate and distribute stresses at the spinal screw-bone interface and increase the pullout strength. With the bone spinal screws in place, the bone should knit properly and as cleanly as possible.

The advent of sterile surgical procedures reduced the risk of infection, allowing doctors to internally set and stabilize fractured bones [1].

An internal fixator may be made of stainless steel or titanium [4], which are durable and strong, with an increasing number of devices being made of Titanium and Titanium alloys because of their lower modulus closer to those of the bone providing less stress shielding, superior biocompatibility and corrosion resistance [5].

Stainless steels are more suitable to use only in temporary implant devices cause they tend to develop a fibrous tissue interface between the spinal screw and bone lowering the removal torque, leading to easier retrieval [6] a disadvantage of the metallic implants is that a second surgery is required to remove the implant. This additional surgery can itself damage the bone and is an obvious inconvenience. The strength of the Titanium alloys is lower to equal to that of stainless steel, but its specific strength (strength per density) is far greater than other alloys. Nevertheless, Titanium has poor shear strength, making it less desirable for bone spinal screws, plates and similar applications [7]. Nowadays, minimally invasive surgery, computer assisted surgery, and in-

troduction of new (biological) implants will certainly find their place in the fracture treatment [1]. These methods decrease the surgical dissection at the fracture site and maintain bone perfusion, to enable a "biological internal fixation"[1].

Currently medicine has two approaches to solve the fixation to the bone problem with or without the use of acrylic cement [8]. A cemented prosthesis is designed to have a layer of bone cement, typically an acrylic polymer called polymethylmethacrylate (PMMA), in between the patient's natural bone and the prosthetic joint component [9].

This technique may offer advantages such has being the quickest way to firmly fix the implant in place by drying up in about 10 minutes. The cement can also prove to be more ideal in extreme cases where the patient has a more porous bone derivative of osteoporosis being more fragile and weak, also it can contain a mixture of antibiotics witch would reduce the risk of infection and possible rejection [10]. However, it has problems of its own since the cement can break down and cause inflammation with the surrounding tissue created around bone-implant interface leading to an eventual loosening of the implant and prompt the need for another joint replacement surgery [11].

The cementless approach does not require the cement and encourages the natural bone to grow in an attempt to increase the longevity of total joint replacement, this biological ingrowth has been used as an alternative to cement fixation [12].

New bone ingrowth is increased in the bead coated or porous-surfaced implants, in contrast to the smooth-surfaced implants. Porous-surfaced implants appear to provide gaps and spaces favorable for interstitial bone ingrowth [13]. Because of its structure, it provides enough gaps and spaces for the chemical (breakdown) products which function as mediators and for bone marrow ingress after surgery, and results in interstitial bone formation.

Grit blasted surface roughening promotes osseointegration and interlocking of remodeled bone matrix directly to the metallic implant surface and, consequently, a mediocre-to-good shear strength as a function of both time and surface roughening facilitating its use of the bare implant without coatings and without bone cement [14].

1.2 Coating Solutions

The unlikeliness of formation of a bone-like apatite layer in body environment deteriorates the bonding strength between the metallic implant and the bony tissues and hinders its long-term application as biomedical material [15][16].

Materials such as Titanium and its alloys have been widely used as dental and implant materials because of their high strength, good mechanical properties and high corrosion resistances, but they do not show very good osteocondutivity [17]. As there is no adherence of the implant material to the bone the actual fixture is limited to the surface area available for the surface pores, relying the fixture on only principles of mechanical retention [17] limiting the highest interface strength to about 30 % of the strength of cortical bone [17].

Many other porous materials however are potential candidates provided that the solid constituents of the matrix. must be sufficiently inert under in vivo conditions to provide favorable conditions for bone ingrowth and have adequate pore size of a diameter conducive to bone invasion and interlock stability meaning a continuous system of pore channels like a matrix all are important requirements for bony ingrowth [18][17]. Also the capability of being manufacturable as thick coatings or thin-walled complex surface assemblies compliance comparable to bone and crack resistant particularly under impact [12].

In 3D multicomponent scaffolds, also known has composites are firstly intended to work as fillers, occupying the available space in the damaged organ/tissue the porous structure, as well as their compositions must promote cellular responses by creating

connective tissue penetrating through the void spaces and channels of porous materials optimizing such characteristics as their adhesion, penetration, differentiation, nutrition, diffusion, and bone in-growth [12][19]. Their programmed bioerosion/resorption activity allows them to provide a framework for growth of new tissue that finally (partially or completely) replaces the scaffold.

Resuming while selecting the material for medical implants, three major factors need to be considered: biocompatibility, osteo-integration and strength [20]. On the other hand an ideal scaffold for bone tissue engineering (BTE) must present the following three main properties osteoconduction, osteogenicity and osteoinduction [21].

Much attention has been given on ceramics that resemble the mineral phase of bone tissue. Hydroxyapatite, octacalcium phosphate and tricalcium phosphate [22] are bioactive ceramics due to the free calcium and phosphate compounds in their surfaces and the resemblance of the chemical and crystallographic structures existent on natural bone, specially Hydroxyapatite [23]. Hydroxyapatite [HAP, Ca10(PO4)6(OH)2] having a composition similar to the mineral phase of bone and tooth enamel up to 50% by volume and 70% by weight of human bone which itself is a modified form of Hydroxyapatite has received continuous attention as biomedical materials to promote accelerated osteointegration, because of its physical and chemical similarities with bone tissues. An interesting finding was that bone grows directly on the Hydroxyapatite surface after 4 weeks, which also was only demonstrated on the Titanium surface after 16 weeks [22].

1.3 Challenges for HAp coatings

However, despite having a high compressive strength the poor mechanical properties of Hydroxyapatite such as the low ductility of Hydroxyapatite limits its application as load bearing materials [19]. One of the main problems in this application is that the Hydroxyapatite itself can only be applied where the mechanical forces are low or only compressive. [24]

Due to their weak mechanical properties porous Hydroxyapatite might fracture if a sudden force is applied them during the healing stage. Cementless fixation technique combines the strength and ductility of metallic implants with the biocompatility and ability to bond to the bone of the Hydroxyapatite [25]. The relatively poor adhesion of pure Hydroxyapatite coating mainly arises from the mismatch of the coefficients of thermal expansion between the Titanium alloy substrate and the Hydroxyapatite coating [26]. Hydroxyapatite already establishes weak interfacial bonds with Titanium substrates implants, the poor bonding strength between Hydroxyapatite and Titanium alloy has been a concern of orthopedists [27][26], due to the risk of having a problem either during surgical operation or after implantation for a given time.

Primary fixation is one of the most important factors in establishing adequate osseointegration between bone and an implant fixture [28]. As such, plasma spraying of Hydroxyapatite and Titanium coatings has been employed to maximize bone formation and rapid stabilization.

1.4 Solutions

Several studies have been made to address this issue of improving the interfacial bond strength of Hydroxyapatite on Titanium based alloys implant materials from graded coatings, bond coats and also composite coatings [13] [15] [29] [30] [31].

Spinal screws coated with osteoconductive materials have optimal fixation strength, proved to be significantly higher than that of the standard spinal screws [28], but suggested that Hydroxyapatite coatings and Titanium coatings are only beneficial for the initial healing period [28] [32]. A study indicated a significantly higher bone contact length for Hydroxyapatite-coated implants as compared to Titanium-coated and Ti implants for both periods tested (12 weeks after implantation and 1 year after loading) in

normal bone [33]. However, this high bone contact length and better osseointegration was not reflected in the pull-out strength as a result of the weak coating– substrate interfacial strength, which proved much higher for Titanium-coated spinal screws.

Another study presented a solution technique which was developed through a monobloc implant with a double coating on a cobalt-chrome (Co-Cr) core for non-cemented fixation [34]. First a coating of commercially pure Titanium was used, on top of which a superficial layer of Hydroxyapatite was applied this double-coating method should provide a long-lasting secure fixation of the implant to the bone. Such a durable bond would be created first by on growth of bone to the Hydroxyapatite layer and secondly, should the Hydroxyapatite dissolve, by the establishment of a permanent bone-titanium bond. Results confirm the hypothesis that a combination of Hydroxyapatite on top of Titanium provides complimentary benefits. Hydroxyapatite results in fast and reliable on growth of bone for secure biological fixation that sustains postoperative weight-bearing [34] [35], and the layer of Titanium secures secondary fixation should the Hydroxyapatite dissolve in the process of acquiring body union [34].

Results of this study supported the choice of this double-coated construct at places where bone marrow was in contact with Hydroxyapatite, this layer tended to dissolve while the Titanium layer remained intact and even showed direct bone ingrowth [34]. Nevertheless, the long-term stability of such coatings is the predominant factor causing the success of the implant [36]. For improving the coating–substrate bond strength and other properties, many attempts have been made to develop biocoatings [37] with higher bond strength. In this case, double layer or multilayer coatings have been considered recently [29][27][15], however it is noteworthy that manufacturing a graded coating with continuous transition of the involved phases onto a substrate with a complex sHApe, like a bone implant with spinal screw thread, is not always feasible [30].

1.5 Composite Coatings

In studies on composites, bonding strength evaluation indicates that Hydroxyapatite/Titanium composite coatings possess much higher bonding strength than the Hydroxyapatite coating, suggesting that the fabrication of Hydroxyapatite/Titanium composite coating is a promising useful way of improving the adhesive strength of the coating and also its cyclic life [13] [27] [29] decrease the residual stress within the top coating, thus improving the mechanical stability of the implant.

Since atmospheric plasma spray (APS) is still one off the main options to create medical coatings and in terms of costs it still proves to be expensive for the complex process of graded coatings [38]. Therefore, a composite coating would be technically feasible and economically viable by replacing the existing alternate layers of HAP/Titanium, can it be done without compromising its properties since it can conserve its phases and using less amount of material of the previous graded method and with lower costs to the manufacturer due to the due to less HAP requirement (HAP~500$/lb and Titanium~80$/lb) [15] and ultimately to the consumer as well.

2

Methods and Materials

1-Materials

2.1 Materials

Three different Titanium batches available at CERAMED SA from suppliers 1, 2 and 3, respectively batch: A, C and D, each with different grades was initially considered for the study. After an initial analysis only one was used for the rest of the study. One batch of HAp designated B from supplier 3 was also used through the whole study.

2- Methods

2.2 Composite Powder Manufacture and Analysis

2.2.1 Titanium and HAp powders initial Analysis

The three different Titanium were compared with a Hydroxyapatite batch from Medipure supplier trough laser diffraction equipment: Mastersizer 2000MU Hidro with water dispersant, repeating 10 cycles. Also a density analysis was performed to all materials with the equipment: AccuPyc 1330 used with Helium gas, repeating 6 cycles so it could be measured with accuracy.

A further visual analysis was performed in order to access the different particle morphologies and sizes the microstructure was characterized under field emission scanning electron microscope (Zeiss Auriga aperture size 5.0 kV WD= 5.3 mm Mag=30.0X Signal = SE2) equipped with an energy dispersive spectrometer (EDS).

2.2.2 Composite Manufacture by Turbula mixing

Turbula Mixing equipment was selected for the manufacture due to its ability to form uniform mixture with materials similar in size, sHApe, and density [39]. The Turbula shaker-mixer can be used in such cases mixing different powder substances with differing specific weights, concentrations and particle sizes in a closed system in homogenously way, using a 3-D spiral motion involving rotation, translation and inversion. This technique also allows the removal of each composite batch mixing container eliminating

cross-contamination and allow for rapid batch changeovers becoming very attractive for commercial use. However lacking on scientific data on the behavior of powders intended to mix, the optimization mixing step typically involves a previous lab work experiment [40].

The Titanium batch most similar in range and density to the available Hydroxyapatite was selected to produce the mixture. Turbula mixing was the method of choice to perform the mixture and Turbula Mixer type T2F 0.18 KW 50 Hz was the equipment used, with a fixed L RPM. Three different mass ratio mixtures 50/50%, 60/40% and 70/30% of Titanium and Hydroxyapatite respectively where tested at 4 different mixing times J1, J2, J3 and JJ3 in order to determine the best dispersion homogeneity of the mixture and the lowest standard deviation so the process could be repeatable without major differences. After the first study the mixture with 60% Titanium and 40% of Hydroxyapatite (w/w) mixed for J3 hours at L RPM was the best one, presenting a black to white contrast ratio close to 3:2, which is the ratio of Ti:HAp present in the mixture. Furthermore, five experiments were made for each of the mixtures and the lowest standard deviation between the ratio of Ti:HAp and the black to white contrast in the optical microscopy images was achieved for 60%Ti/40%HAp.

2.2.3 Titanium and HAp Mixing Analysis

These mixtures were analyzed by an inverted optical microscope Olympus IX-81 equipped with a set of high-quality objectives of 5 X and with the help of image edition software ImageJ. Post-processing of the images was carried out using the Image J software. By cropping the initial image from the microscope, its brightness and contrast were increased in order to eliminate interferences and easily identify each material regarding contrast ratio associated with the different coloring of both Hydroxyapatite (white) and Titanium (black). Then, the image was converted into a binary image using a suitable threshold to extract the ratios between black and white from the background. These steps were accomplished through measurement of the area fraction of the different materials in the image using the measurement analysis toolbox in Image J.
The microchemistry dispersion of the mixture was then qualitatively characterized under field emission scanning electron microscope Hitachi TM 3030Plus Tabletop with aperture size 15.0 kV WD= 8.7 mm Mag=80.0X Signal = SE2, equipped with an energy dispersive spectrometer (EDS).

2.3 Composite Coating Manufacture by Atmospheric Plasma Spray

After the Turbula mix analysis a pre-selected powder mix of 60%Ti40%HAp was then subjected onto the APS system and several off its parameters were pre chosen and fixed in order to access if the mass ratio was maintained after the Turbula mixing and ultimately after the mixture been submitted trough the APS (Atmospheric Plasma Spray) system onto the substrate, in other words if the mixture dispersion would be maintained from powder mixture into the composite hard coating composition. Using the pre-selected powder mix an initial coating was produced using APS system (Sulzer Metco, Swizerland), using program parameters in table 1 bellow.

Table 1-Initial parameters for APS program 1 standard values

PARAMETERS	UNITS	VALUES
Current	A	Z
Primary Gas Flow	NLPM	V (Argon)
Secondary Gas Flow	NPLM	X (H_2)
Spray Distance	mm	R
Carrier Gas Flow	NLPM	T (Argon)
Powder Feed Rotation	%	W
Powder Feed Vibration	%	Q

2.3.1 Composite Atmospheric Plasma Spray Coating Analysis

Using the pre-selected powder mix choose in the last cHApter an initial coating was produced using APS program parameters in table 1 bellow. Using a different SEM equipment Phenon PRO-X an EDS (semi-quantitive) analysis of element content was performed. Based on the energy spectrum of the atomic transitions L-alpha (Lα) and K-alpha (Kα) [41], for Titanium and Calcium. This way for each element it was generated a close Atomic content that could be appreciated in order to determine if the powder mix would suffer any influence on its mass ratio after being submitted trough APS system under table 1 parameters.

After the SEM-FRX analysis on the coating it was possible to confirm a very close atomic mass content of Titanium (Ti) and Calcium (Ca) to the mass ratio to the mixture and define the 60/40% ratio has our target mixture for further studying.

2.4 Preliminary study

A preliminary process investigation was carried out. The investigation of direct influence presented by the variation of each pre-selected parameter. Parameters were chosen based on previous literature and equipment limitations. All parameters based on the standard program 1 parameters, and increased and decreased from this point until either the equipment limit was reached or until a viable coating was not produced. Each parameter was then varied separately while setting the remaining parameters at set central values, these were all easily adjustable and easily controllable

All initial APS parameters[1] were fixed however some of the primary parameters has shown in table 1, were one by one changed in order to access their direct influence on properties like crystallinity, thickness, roughness and coating adhesion strength.

Table 2-Primary APS parameters used for challenging in the preliminary study

APS PROGRAM 1		
Parameters	Units	Values
Current	A	Z
Spray Distance	mm	R
Primary Gas Flow	NLPM	V (Argon)
Secondary Gas Flow	NLPM	X (H_2)

The parameter range, was first investigated in order to select suitable levels in order to optimize the production of composite 60%Ti40%HAp coatings. The preliminary coatings produced in this study were compared to the original Hydroxyapatite feedstock powder.

The three main properties analyzed in the coating were crystallinity, adhesion strength and roughness. The roughness of surface analysis was performed in order to understand the degree of melting of the particles during the coating process, and if their size contrast would differ and influence the difference between the highest and lowest peak, with the challenging of parameters. The crystallinity of the coating was measured also one of the most of the most important properties affecting the dissolution rate of Hydroxyapatite coatings and are strictly controlled by the FDA [42]. The adhesion strength was also measured since it is the property that it is imperative to improve. Also a visual appreciation was done in order to see the presence of Hydroxyapatite or its decomposition by the lack of white coloring in the coating.

Visual evaluation was performed on stainless steel type 316 plate-like (Ø 25 mm) samples. The content of HAp that adhered to the coating was visually accessed by comparing with the same samples after G type of acid vol.65% treatment witch dissolves calcium phosphates without damaging the substrate and the Titanium.

[1] The description of APS technique, its primary control parameters and their influence on coatings properties are discussed in Annex I.

2.4.1 Preliminary study- Description of coating characterization techniques

a) Crystallinity - XRD Coating Analysis

Disc sHAped stainless steel substrate were used, plate-like (Ø 25 mm) for micro structure observation, phase analyses and crystallinity. The phases present in the coatings were identified using X-ray Diffraction (XRD). Scans were carried out using the XRD, X´Pert Pro PANalytical Difractometer. The parameters used are given in table 3.

Table 3-XRD parameters conditions for analysis.

PARAMETER	VALUE
Range (2Θº)	8.007999996 - 80.000146754
Scan Type	continuous
Scan Speed (sec/step)	0.0167113
Divergence Slit (mm)	0,76
Anode material	Cu
K-alpha 1 wavelength (λ)	1.5405980
K-alpha 2 wavelength (λ)	1.5444260
Generator Voltage (V)	40
Tube Current (mA)	45

X-ray diffraction patterns were also used to determine the % crystallinity of the HAp powder and then used to compare against the coated Ti/HAp composite. This was calculated using the area of crystalline peaks in the region 25 to 50 º 2θ and the area of the amorphous diffuse background in this region. The areas of interest were already predetermined using ISO 13779-3. One XRD scan was carried out for each coating and the crystallinity calculated for each sample. The Relative Intensity Method involves comparing the intensity of fully crystalized reference compound (uncoated HAp) peak for the different XRD patterns. By comparing the integrated area intensity of the HAp peak coating with the integrated area intensity of the peak of a standard HAp uncoated material, in its more crystalline form. The determination of properly crystallized phase is based on the measurement of the Integrated Intensity of ten lines, suitably chosen. Due to the presence of Titanium in the powder mix and in the coating it was not feasible to remove the coating, crush it under 40 µm and analyze it in the form of powder the way It is done with single HAp coatings, so it was decided to analyze the coating in the "parallel beam

geometry" with grazing Incidence X-Ray. Both methods were previously tested and presented similar values for the coated single Hydroxyapatite. Although the Relative Intensity Method results are not considered to be as reliable as other methods, but are a good fast analogy of how the APS process is affecting the properties of the coated material.

b) Coating Adhesion Maximum Strength

Cylindrical (Ø25.4 mm in diameter and 50 mm in length) stainless steel pieces were used for bonding strength measurements according to ASTM F1147-5. APS system (Sulzer Metco, Switzerland) was applied to fabricate Hydroxyapatite/Titanium composite coatings under modified spray parameters listed in Tables 11, 12, 13 and 14. Pure Hydroxyapatite coating was also fabricated for comparison. The thickness of the coating tested has to be enough to ensure that the bonding agent cannot penetrate all the way through the coating to the substrate, this is determinate preliminary testing. The coating thickness for all specimens was about around 100 ± 30 µm and all specimens were grit blasted before with Al3O2 (Alumina) particles (grain size of 60 mesh at 5 bar pressure, 75° angle, and grinding time 1 min following a grit blast with grain size of 20 mesh also at 3 bar pressure, 75° angle, and grinding time 2 min according to previous studies. Reaching a roughness average $R_{a,}$ between 3-7 µm this was performed in order to improve substrate surface adhesion of the coating by enhancing superficial area and eliminating possible oxides formed that can influence also the coating adhesion, facilitating mechanical anchoring of the Hydroxyapatite-Titanium composite.

The bonding strength of APS composite coatings to the substrate was evaluated in accordance with ASTM F1147-5 using an Instron-type universal test machine (Instron 4507) at a crosshead speed of 0.25 cm/min. Two identical cylindrical Stainless steel type 316 were used as a set. Both sides of deposited samples were glued to the shafts using instant adhesive glue (American Cyanamid Company, FM 1000). The specimens were also cleaned with high pressure compressed air after grit-blasting to remove loose alumina from the blasted surface. The assembled samples were placed in an oven at 176 ^{0}C for 3 h for thermal curing. Five samples were tested at each time and the average value was presented

c)- Surface Roughness

The surface roughness of the coatings was determined using a Mitutoyo Surftest SJ-410 surface roughness tester using the parameters outlined in the table below. Three measurements were carried out for each coating and an average was presented.

Where Ra is the arithmetical mean of the absolute values of the profile deviations, Rt is the total height of the roughness profile: Difference between height Zp of the highest peak and depth Zv of the deepest valley within the evaluation length. Rz is the mean value of the difference of the vertical distance between the highest and deepest profile point.

Table 4-Roughness measurements parameters conditions for analysis

PARAMETERS	VALUES
Norm	ISO 1997
Λ_c Cutt off value	8 µm, $R_a \leq 80$ µm
Λ_s Cutt off length	2,5 µm
Surface Profile	Off

2.5 Parameter Level Selection

After the preliminary study was carried out, based on knowledge of the equipment limits and on parameter levels reported in literature [42] [43] [44]. A results analysis was performed and then pre-selected levels were chosen based on the range of best results presented for each parameter challenged, the so called low and high levels were set within the acceptable process limits identified. The parameter selection was based on crystallinity influence criteria, since it was a critical property to address and adhesion strength results were overall with good results during the preliminary study.

2.6 Screen Testing by Design Off Experiments- Full factorial with 2 levels

A 2^k full factorial design for four independent variables A-Plasma Power, B-Nozzle Distance, C-Primary Plasma Flow and D-Secondary Plasma Flow was performed with a total of 16 sets of experiments was chosen with one replica for each experiment, adding a total of 32 experiments designed randomly by Statistica software.

In this design, the factors were varied at two levels – low and high. The measured output from the experiment was equaling to the "crystallinity of the coating". Once the experiment was run, the effect of each factor was evaluated by contrasting the average response when the factor was not changed with the average result when it was changed.

The best set of levels was discriminated for each factor, following the predicted range of values was also calculated[2]. A confirmation experience was also done.

[2] A more detailed description is present in Annex II

3

Discussion and Results

3.1 Material Analysis

3.1.1 Powder size dispersion Analysis

Powder size dispersion is one of many variables that can influence the quality of the plasma-sprayed coating due to its volume and mass response to the high heat extraction that is inherent to plasma thermal spraying. Both Titanium and Hydroxyapatite have high melting temperatures, respectively 1850 ºC [30] and 1650 ºC [45]. It is important that both their range sizes are the most similar as possible allowing them a good uniform mixture using the Turbula mixer, but also because for them to behave close to one another under the same APS conditions. One APS parameter the powder carrier gas flow will assume a value that must be suited to inject into the system both for Titanium and Hydroxyapatite powders at the same rate. Avoiding a big mismatch in the different materials sizes and densities is very important when it comes to mixing them. It is recommended to use powders with a particle size ranging from 20 to 100 µm [46], since below this range powders can solidify even before they reach the substrate being later embedded in the laminar structure and may lead to a drop of adhesion instead of improving it. Despite these facts, issues concerning the incorporation of solid particles by the coating can always be addressed and optimized by adjusting operational variables such as the distance from the torch to the substrate, primary/secondary gas flow, and electric current in the plasma.

Three different commercially available Titanium batches and grades were compared (Figure 1) with the Hydroxyapatite batch trough laser diffraction equipment: Mastersizer 2000MU Hidro with water dispersant, repeating 10 cycles so it could be measured with accuracy.

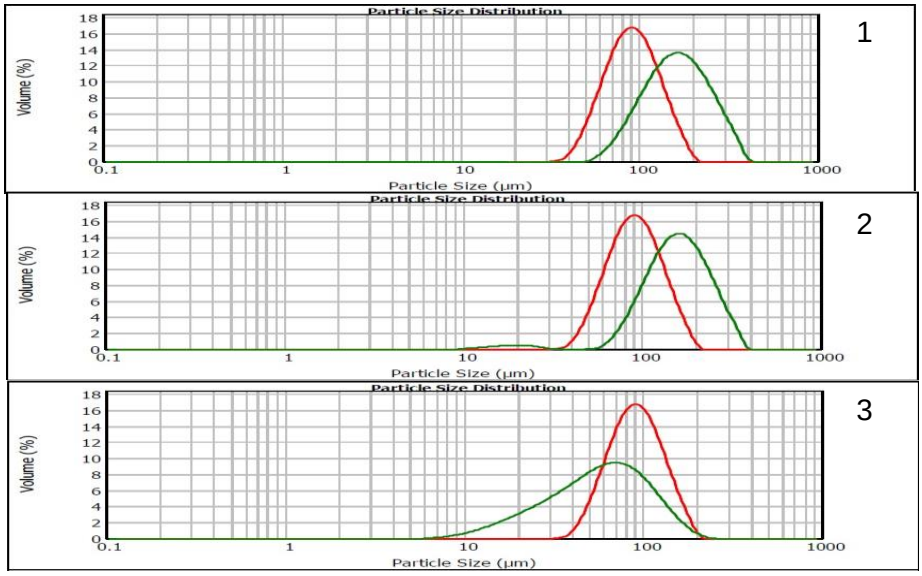

Figure 1-Comparison image between the three range size graphs from batches of Ti in green and the HAp batch in red. Chart 1 batch: C vs B; ,chart 2 batch:D vs B and chart 3 is A vs B.

All Titanium powders present a broader size distribution, with batch: C presenting a very uniform normal distribution, however there is a big mismatch between its range and that of the HAp powder. Batch: D presents a little peak at 20 µm size and extends long until the 400 µm in size being a very wide range to take into account. Batch: A presents the closest particle size range to batch B, with particles being distributed between 5 and 200 µm at a relatively normal distribution.

3.1.2 Titanium and Hydroxyapatite Powder Density Analysis

Both density gas pycnometry analysis and particle size analysis by laser diffraction were performed in order to determine the materials properties and their viability to work together as a mixture composite.

From previous literature it was possible to access that Titanium density was of 4.5 g/cm^3 [47] and Hydroxyapatite was 3,15 g/cm^3 [48] which were then confirmed by analysis done using Picnometry equipment: AccuPyc 1330 used with Helium gas, repeating 6 cycles so it could be measured with accuracy. Results are shown below on table 5.

Table 5- Density analysis results for all three Titanium batches and HAp batch

MATERIAL	BATCH	AVRG VOLUME cm3	STDV cm^3	AVERAGE DENSITY g/cm3	STDV g/cm^3
HAp	B	1.0545	0.0023	3.1483	0.0069
Titanium	A	1.6675	0.0020	4.5220	0.0053
Titanium	D	2.0873	0.0044	4.5250	0.0095

Titanium	C	2.2356	0.0019	4.4826	0.0039

Titanium powder batch: A presents the closest density to HAp batch: B. This is pretentious since generally, materials similar in size, sHApe, and density are able to form the most uniform mixtures [39] when mixed by Turbula mixer.

3.1.3 SEM Powder Characterization

A SEM analysis was performed on different raw mixing materials from Hydroxyapatite to all three batches of different Titanium powder particles, as a complement of the particle size analysis allowing perceiving the mismatch of sizes and sHApes.

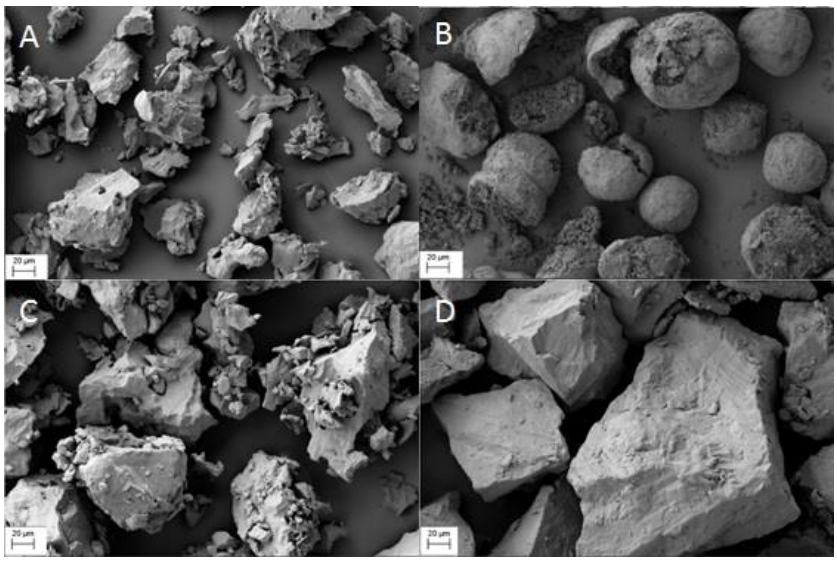

Figure 2-A-Ti batch: A; B - HAp batch: B; C- Ti batch C; D-Ti batch: D.

When it comes to its morphology observed in Figure 2, the Titanium powder particles are irregular in sHApe and many particles have sharp sHApe and irregular surfaces. All Titanium batches are really irregular with lots of tips comparing with the smooth sHApe of the HAp that in the most part resemble spheres. All Titanium small particles are agglomerated and form relatively large clusters where some include larger sized particles. This observation yet is not so clear with Titanium batch: C, but with the other two batches some agglomeration between particles is observed with smaller particles of Titanium surrounding bigger ones in batches A and D; in fact, no larger particles without attached small particles were detected in the acquired SEM images.

At first sight becomes clear that the Titanium batch closest to the range of the HAp is A.

From this point only the Titanium Batch A was considered for the following study since it was the only one with a closest size range and density values to that of the Hydroxyapatite Batch B from supplier 3 available at the CERAMED facilities in the time of this study.

3.2 Composite Manufacture and Analysis

A Turbula preliminary lab work was done in order to determine the best uniformly achievable mixture. Three different ratio mixtures where tested at different mixing times in order to determine the best dispersion homogeneity of the mixture. All of them used the supplier 1 batch: A Titanium and supplier 3 batch: B Hydroxyapatite. Based on previous literature the best range for the HAp-TiO2 composition is somewhere in between 47% and 57% volume for the addition of Titanium to Hydroxyapatite [49]. Therefor three close mass ratios displayed on table 5 below were tested at different mixing times, in order to find the best (with the lowest standard deviation).

Table 6- Ti/HAp Mass ratio vs Aproximal Volume ratio

MASS RATIO TI/HAP (%)	APROX.VOLUME RATIO TI/HAP(%)
70/30	61
60/40	52
50/50	42

The equipment Turbula Mixer type T2F 0.18 KW 50 Hz was used with a fixed rotational speed of L RPM and all the mixtures were done using the same amount of total mass and the same type of container was used for all of them, meaning that only one parameter was available for testing, time (h).

3.2.1 Optical Microscope Analysis

These mixtures were later analyzed by optical microscope Olympus IX-81 and with the help of image edition software ImageJ, analyzing contrast ratio associated with the different coloring of both HAp (white) and Ti (black) and later with SEM imaging for confirmation.

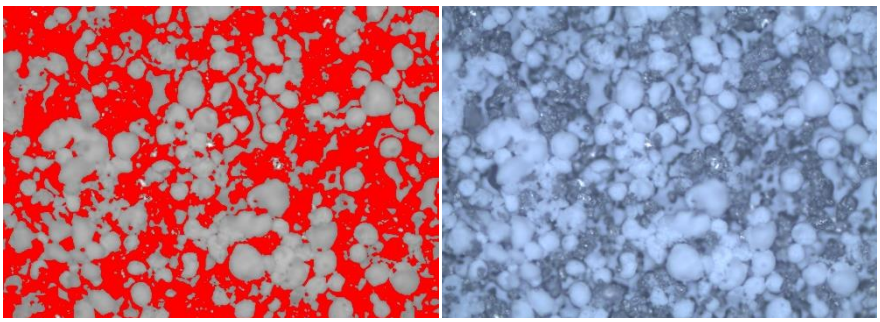

Figure 3.-Optical microscope image of Ti/HAp respectively 40/60% mass ratio after 4 hours in the Turbula Mixer. The same image, on the left after submission to contrast analysis on Image J software on the left, and on the right the same original image.

Using this analysis and testing several different mixing timings it was possible to access and to evaluate in terms of homogeneity of the mixture, and of repeatability standard meaning the lowest standard deviation.

These steps were accomplished through measurement of the area fraction of the different materials in the image using the measurement analysis toolbox in Image J. The approximation between mass ratio and area ratio is expected, off course this is not the most accurate method, but for an initial study is suited. Both powders were mixed in a Turbula Mixer for J1, J2, J3 and J4 h with different Ti/HAp mass ratio.

Table 7-Different Turbula mixing times and Ti/HAp ratios results by calculating the ratio of white area over the black using Image J software.

	50Ti50HAp% MASS	**60Ti40HAp% MASS**	**70Ti30HAp% MASS**
J1h mix	44,18 ± 2,88	45,35 ± 2,74	37,81 ± 2,96
J2h mix	49,84 ± 4,48	49,62 ± 2,50	38,82 ± 3,18
J3h mix	51,73 ± 2,86	42,90 ± 1,78	41,09 ± 3,76
JJ3 mix	55,81 ± 2,53	39,76 ± 3,22	31,40 ± 8,40

The best results showed to be the 60%Ti40%HAp mass mixture with J3 hours in the Turbula mixer at L rpm, with a similar white coloring area to the expected mass ratio of HAp and a considerable low deviation. For that reason, it was chosen to be the ratio to proceed with the study since it would presumably present less amount of error associated and the most accurate mix in terms of repeatability

.

3.2.2 SEM Analysis Powder Mixing

The morphology and chemical elements were also analyzed under field emission scanning electron microscope (Zeiss Auriga aperture size 15.0 kV WD= 8.7 mm Mag=80.0X Signal = SE2) equipped with an energy dispersive spectrometer (EDS).

It is clear from figures 4 and 5 a reduction of the presence of Ca in yellow (right up) content and an increase of Ti in green (right down), confirming the increase in Titanium in the mixture.

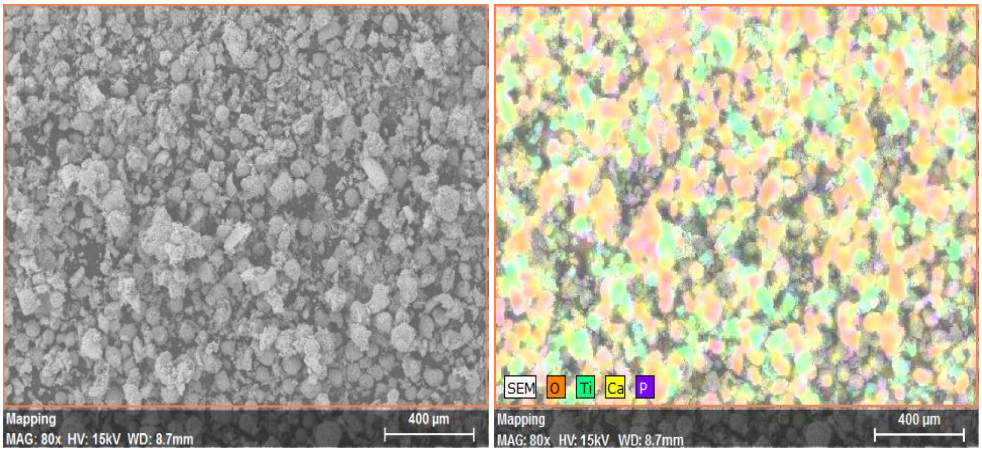

Figure 4- 50%Ti50%HAp composite powder after J1 hours in the Turbula SEM analysis

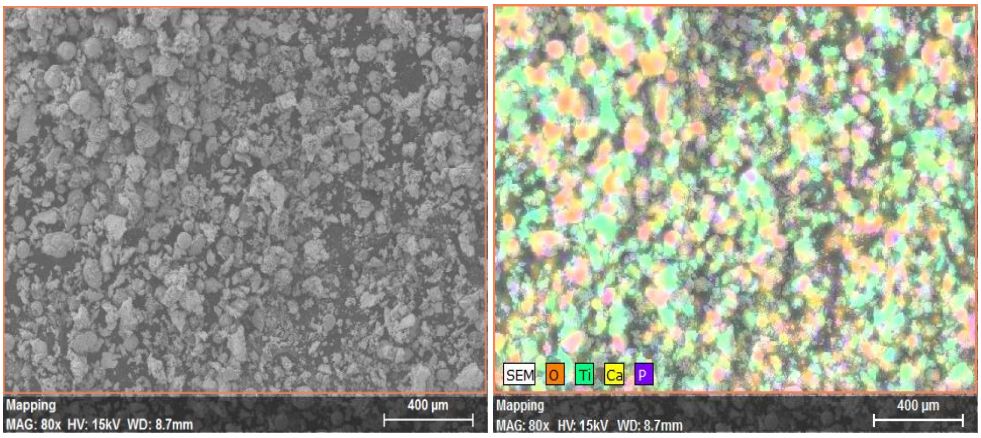

Figure 5- 70%Titanium30%HAp after J1 hours in the Turbula composite powder SEM analysis

3.2.3 SEM FRX Analysis of a APS Coating using the pre-selected composite powder

Using a different SEM equipment Phenon PRO-X a more powerful and precise analysis could be made in order to determine if the powder mix would suffer any influence on its ratio material dispersion after being submitted trough APS system using the listed parameters on the table 1.

The selected powder mix (60%Ti/40%HAp) was then subjected onto the APS system and several off its parameters were fixed with values listed on table 1. The objective was to access if the mass ratio was maintained after the Turbula mixing and ultimately after the mixture been submitted trough the APS system onto the substrate. It was also useful to track any element contamination after passing through the whole system and process.

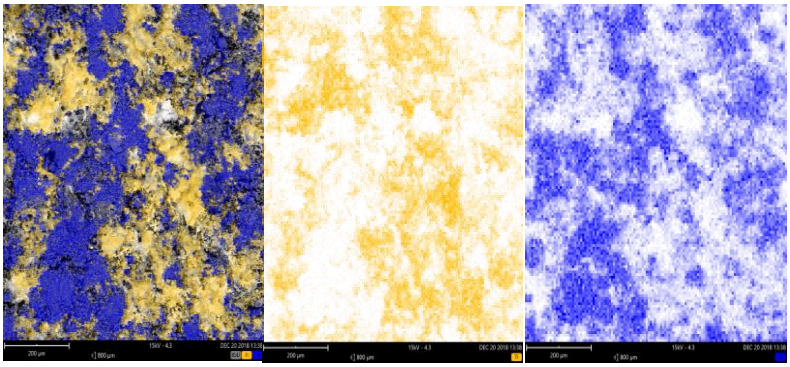

Figure 6-On left 60%Ti40HAp powder mix coating; middle image in yellow is the Titanium content and in the right image the blue represents the Calcium content. Original SEM image conditions: FOV: 800 µm, Mode: 15kV - 4.3, Detector: BSD Full

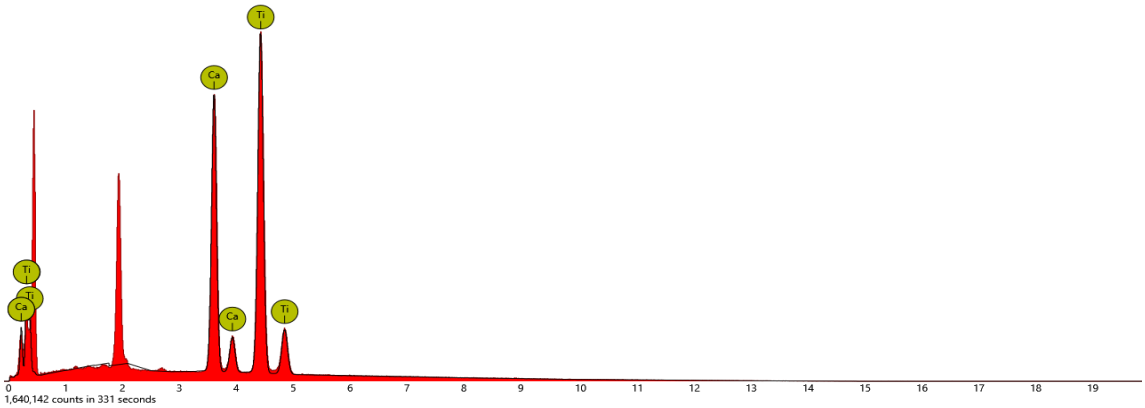

Image 1- Fluroscence X-Ray diffraction analysis with disabled elements: B, Ce, Er, La, Lu, Nd, O, Pr, Tm.

Table 8-SEM Fluroscence X-Ray diffraction analysis results.

ELEMENT SYMBOL	ATOMIC CONC.	WEIGHT CONC.	OXIDE SYMBOL	STOICH. WT CONC.
Ti	63.88	67.87	TiO_2	71.57
Ca	36.12	32.13	CaO	28.43

Based on table 8 atomic content mass values a similar content of Titanium and Calcium to the mass ratio used in the APS system 60%Titanium and 40% HAp is observed. Taken the fact that HAp is a material primarily constituted by a matrix of calcium, other minerals and organic compounds [50]. This approximation was accepted to determine a close content in the coating constituents and the original constituents of the composite powder, without any major changes that would at this stage compromise the following study.

3.3 Preliminary study of APS parameters direct Influence on coating properties

Before the beginning the Design of Experiment study, a preliminary process investigation was carried out. Since the coating first analysis was performed using a Titanium

standard program 1, a need to understand how each parameter would influence the coating properties was done. Optimization is only possible if an understanding of the process parameters is achieved, and then used in order to reach the best coating properties possible. The investigation of direct influence presented for each parameter was started at the central value, based on the standard program 1 parameters, and increased and decreased from this point until either the equipment limit was reached or until a viable coating was not produced. After literature investigation [42][47][51][52] [53] only 5 parameters (Power, Distance, Primary Gas Flow, Secondary Gas Flow and Powder Gas Carrier Flow) were considered important to change in order to improve our coating crystallinity and adhesion, however one of the parameters had contradicting information on literature. Powder Gas Carrier Flow where some say it would influence only the coating thickness [42], and others still were using it as influential factor in their studies. A confirmation test was made were HAp, Titanium and the 60%Ti/40%HAp composite were coated with the same conditions and the final thickness was compared between the three samples. The same program 1 was used with the carrier Gas Flow at a value T NPLM of Argon and W% rotation and Q% vibration to the Stock Feeder. Results are shown at figure 7 below.

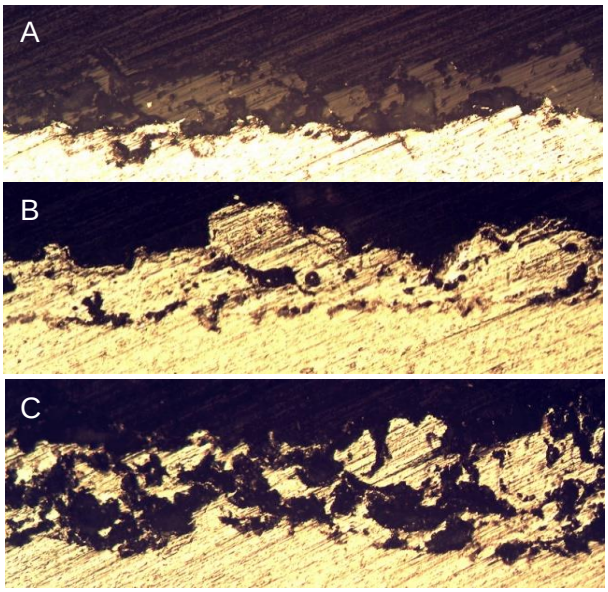

Figure 7-Thickness of HAp (A), Titanium (B) and 60%Ti40%HAp (C) composite layer, using the same Stock Feed rate, Powder Carrier Gas Flow and robotic arm cycles. Picture taken by Microscope Olympus IX-81 Mag. 20x off a laminar cut of stainless steel substrate and coating encapsulated on an epoxy mold

None of the materials presented significant average thickness changes from one another, so it was concluded that both values for Powder Carrier gas flow and Stock feeder vibration and rotation were to be fixed using T, W and Q respectively. These parameters were fixed, therefor unaccounted for in the preliminary challenging allowing to reduce the number of experiences required. The number of cycles has no profound effect on the considered responses, it can only be used as a factor to achieve different coating thicknesses [52], so it was also fixed.

Also when appreciating all three different coatings on figure 7, is possible to observe that the HAp coating presents a smooth almost continuous coating thickness following the substrate profile. Contrasting the single Titanium coating presents some high peaks and valleys, even though both coatings present an equivalent thickness averages the R_t between both presents some discrepancies. This phenomenon is due to the existence of particles that did not melt trough until the core and did not "splat" into a laminar profile. The composite coating presented a more uniform coating profile however the presence of Titanium still shows that its influence on the R_t is considerable.

Table 9- Coating crystallinity values for HAp coated (APS) and uncoated (powder form)

Material	Crystallinity Values
HAp uncoated	>95,00 %
HAp coated	>45,00 %

Analyzing table 9 is possible to observe a general peak intensity decrease in the HAp coated compared to the uncoated.

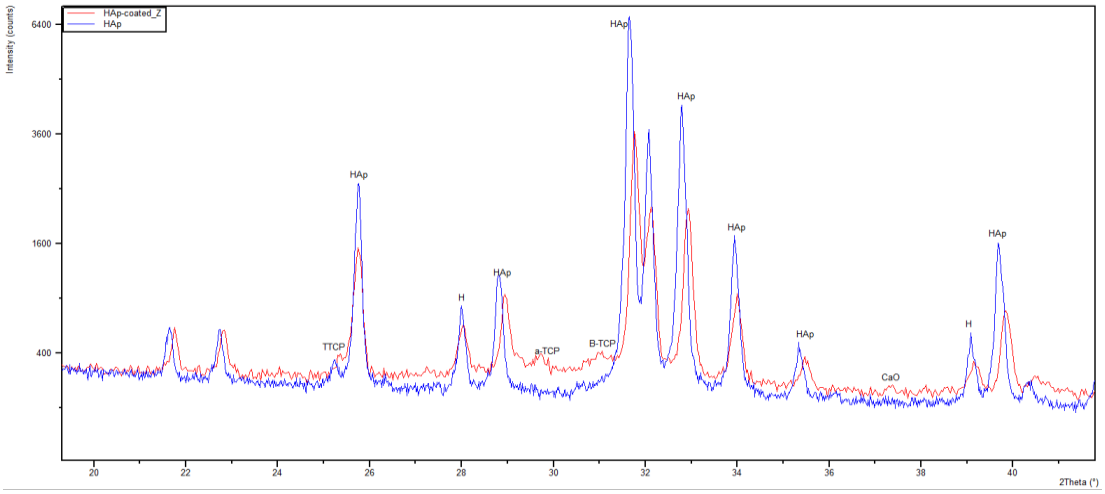

Figure 8-Peak phase location and difference between coated and uncoated HAp

Observing image 9 above, its noticeable a decrease in overall phase peaks. Also many TCP phase peaks and CaO phase peaks rise or appear has a sub result of the decomposition of the HAp appear because of the thermal energy imposed on the material. This is due to the high temperature of the plasma jet and enthalpy promotes, even during short residence times of the HAp particles on the "flame", a considerable decomposition [51].

Table 10- Current Adhesion strength values for HAp, Titanium and 60%Ti40%HAp using standard values for program 1

Material	Adhesion Strength Value
HAp coated	16,3 MPa
Titanium coated	30,0 MPa
60%Ti/40%HAp	20,9MPa

Using standard program 1 values from table 2 all three powders were submitted trough the APS system using the same conditions. All results for adhesion strength were presented on table 10 above. Where HAp presents a strength slightly above the required minimum (>15 MPa weak), and single Titanium considerably above this value and also the metallic standard requirement (≥22 MPa). On the other hand, the composite coating presented an in between of both requirements value, above the ceramic coating minimum but under the metallic coating minimum.

3.4 APS Power parameters settings

Table 11-Analysis results for variation of Plasma Spray Power supplied levels

Parameters **Program 1 Variation of Power/Current Supply distance**					
Levels	1	2	3	4	5
Parameter Values (A)	Z_{-2}	Z_{-1}	Z	Z_1	Z_2
Crystallinity (%)	26,34	29,69	20,34	25,80	21,05
Adhesion (MPa)	11,46 ± 3,49	21,96 ± 2,63	19,08 ± 2,45	26,27 ± 3,70	11,56 ± 3,25
Thickness (µm)	150	180	175	220	200
Average roughness R_a (µm)	R_a = 8,39 R_t = 40,94 R_z = 33,11	R_a = 8,92 R_t =53,45 R_z =47,64	R_a = 9,32 R_t =72,88 R_z =64,56	R_a = 10,31 R_t = 100,94 R_z = 85,24	R_a = 13,21 R_t = 89,17 R_z = 69,15
Respective Image	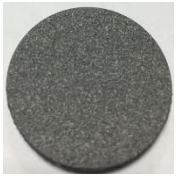	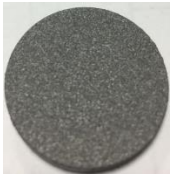	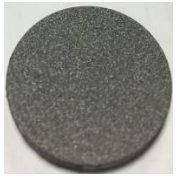	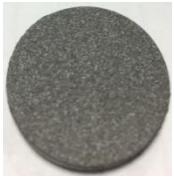	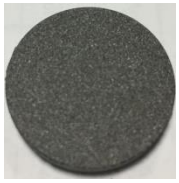
Respective Image After G Type Acid vol. 65% treatment					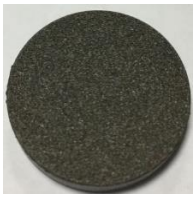

Analysis results for variation of Plasma Spray Power supplied are shown in table 8 above. Where Power is proportional to current. With lower plasma power, a large number of particles were only little melted so that they bounced off on impacting the sample surface. This is noticeable in the samples thickness witch is rising with the power level, also by recording R_z.it is also clear that the Individual size of the particles also increased with the power until a current value of Z_2; after this probably the temperature was too high and particles fully melted into a liquefied state decreasing the average thickness since they spread more on the surface, with a hotter nucleus core. Also it is clear the decomposition of the HAp at Z_2 in the visual aspect to the sample; the lack of white in the coating material color is an indicator of the decomposition of the HAp and directly related to the temperature it was subjected to.

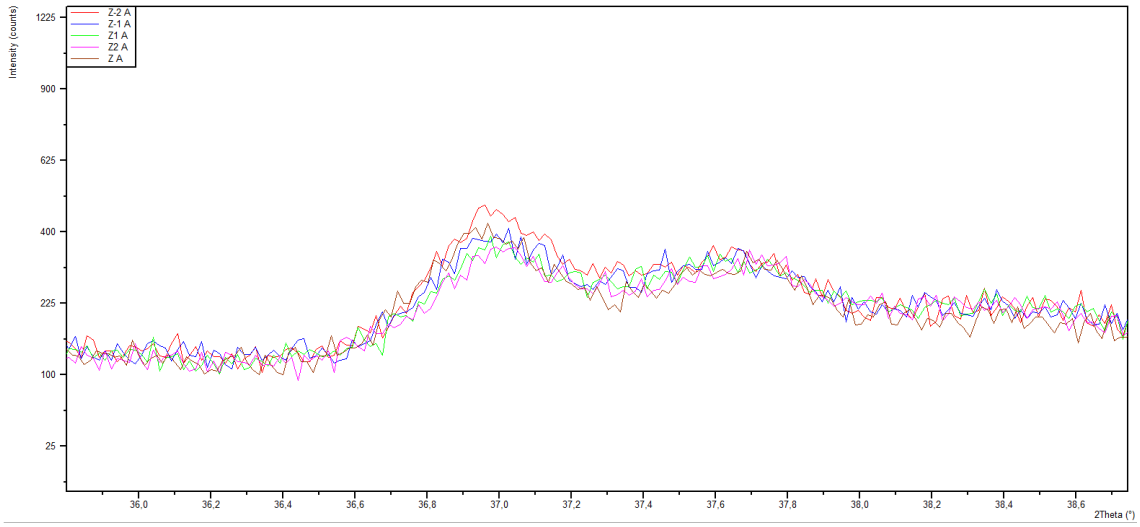

Figure 9-Influence of Plasma Power supplied influence on the CaO peak

High current or power level caused an increase in particle temperature and velocity [42,51]. Increased power or current was found to lead to a decrease in the purity and crystallinity of HAp coatings [29], wich can be observed on crystallinity values at table 11, decrease has power supplied is increase. On figure 9 however the Cao phase peak does not present significant changes has the values change, there is a tendency for the peak intensity to rise with the Power supplied values, but it can be said that its influence is low.

3.2.2 APS Spray Gun Distance parameters setting

Table 12-Analysis results for variation of Spray Gun Distance levels

Parameters
Program 1 Variation of Spray Gun Distance

Levels	1	2	3	4	5
Parameter Values (mm)	R_{-3}	R_{-2}	R_{-1}	R	R_1
Crystallinity (%)	X (burned)	20,45	21,25	19,46	19,39
Adhesion (MPa)	X (burned)	14,69 ± 3,06	17,54 ± 2,92	19,64 ± 2,68	15,08 ± 3,19
Thickness (µm)	X (burned)	200	190	165	80
Average roughness R_a (µm)	X (burned)	R_a = 8,67 R_t = 55,21 R_z = 44,02	R_a = 9,55 R_t =69,09 R_z =55,81	R_a = 9,67 R_t = 53,72 R_z = 42,34	R_a = 9,36 R_t = 55,21 R_z = 49,60
Respective Image	X (burned)	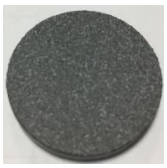	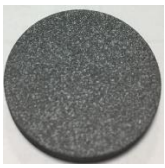	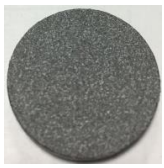	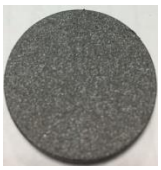
Respective Image After G Type Acid vol. 65% treatment	X (burned)	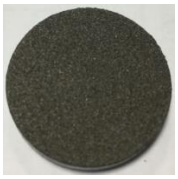	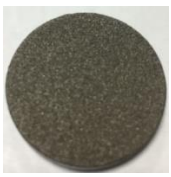		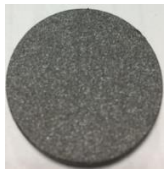

The proximity of the "Plasma flame" affects the travel time of each particle during their "flight" and so their ability to receive thermal energy and transition from their solid state to a semi-liquid/molten or even completely melted state. Observing figure 10 below it is clear that at R_{-2} mm distance the flame to the substrate allowed for less decomposition than at R mm since the CaO phase peak showed a decrease in its area. The temperature of the substrate and the coating is also influenced by this parameter, since the closer the nozzle the and more of the heating on the substrate maintained at a higher temperature. This allows recrystallization of the sprayed coating to occur [42] the contrary will result on a more quickly and a more amorphous coating. This is more evident when observing the crystallinity behavior when challenging the distance at table 12.

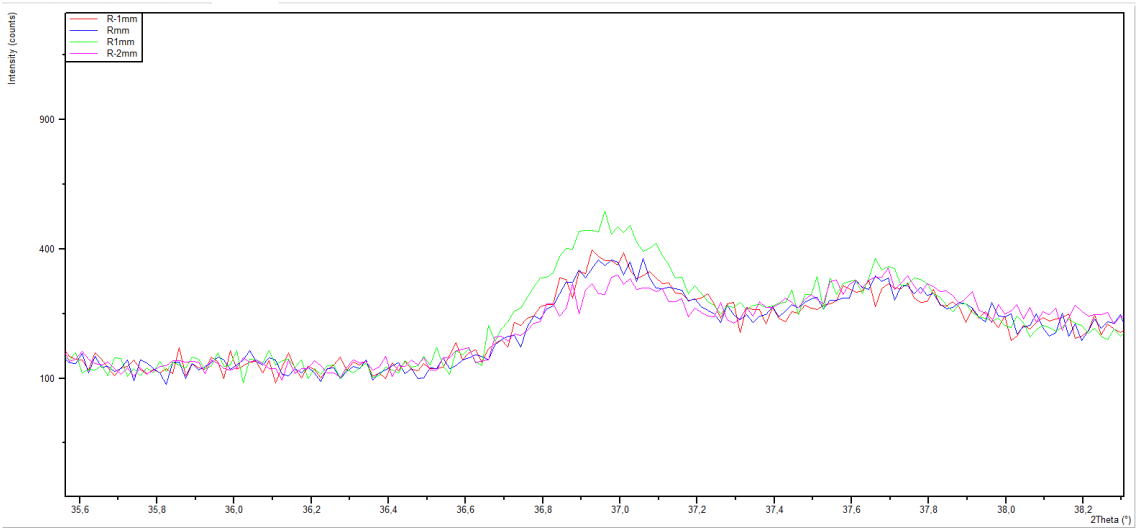

Figure 10-Plasma Spray gun distance influence on the CaO phase peak

3.2.3 APS primary Gas Argon parameters settings

Table 13-Analysis results for variation of Argon Gas Flow levels

Parameters **Program 1 Variation of Argon Gas Flow**					
Levels	1	2	3	4	5
Parameter Values (NLPM)	V_{-2}	V_{-1}	V	V_1	V_2
Crystallinity (%)	10,75	12,48	23,34	28,35	32,07
Adhesion (MPa)	25,37 ± 3,01	20,23 ± 2,72	19,78 ± 3,11	15,51 ± 4,02	10,73 ± 3,86
Thickness (μm)	210	180	175	100	90
Average roughness R_a (μm)	R_a = 10,24 R_t = 76,40 R_z = 57,46	R_a = 10,08 R_t = 64,65 R_z = 62,65	R_a = 7,73 R_t = 55,02 R_z = 49,15	R_a = 7,08 R_t = 47,50 R_z = 42,10	R_a = 7,35 R_t = 49,53 R_z = 40,96
Respective Image		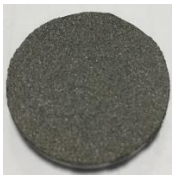	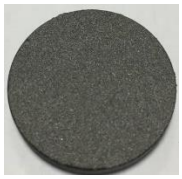	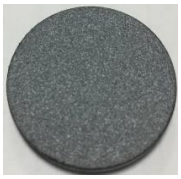	
Respective Image After G Type Acid vol. 65% treatment	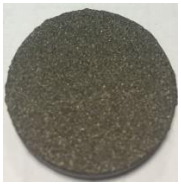	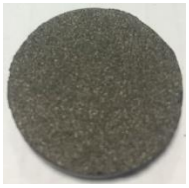	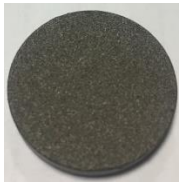	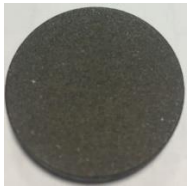	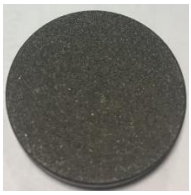

Analyzing the results shown at table 13 above, for all levels except when V_2 NPLM of Argon, adhesion strength is higher than single HAp values. However best crystallinity values are precisely at high flows of Argon. Starting from V NPLM of Argon only smaller Titanium particles managed to coat the substrate, since when rising the flow there is a considerable drop in the coating thickness. This last fact indicates that probably a number of Titanium particles having a higher point of fusion do not absorb the heat to the point of melting. By appreciating the Ra roughness of the surface becoming more smooth the higher the flow meaning that smaller particles are increasing their presence, or the reverse bigger particles are less present in the coating. This has to do with the flame relation between Argon and H_2, since the higher the H_2 content the more powerful the flame reaching a higher temperature. By analyzing Rt where a drop between the highest and deepest point reveals that only smaller particles are “melted” since the bigger particles bounce off decreasing the difference between highest and deepest point. A large number of particles were only partially melted or not melted at all so that they bounced

off on impacting the sample surface, this became more obvious with the larger Titanium particles, every time the flow increased less large particles received sufficient energy for melting, meaning when they reach the substrate they would bounce off. The ratio between primary gas and secondary is important as well since the higher this ratio the less thermal energy, and the less decomposed the HAp gets.

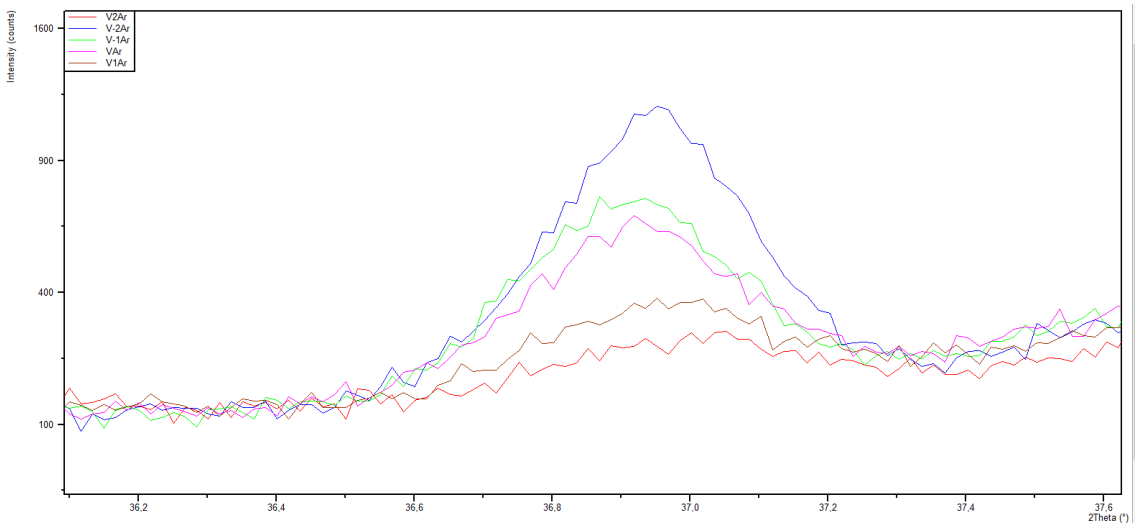

Figure 11-Argon flow challenging influence on CaO phase peak

At low Primary Gas flow and with the presence of fixed secondary gas H_2 the ratio between the gases gets higher and at high plasma jet temperatures, even if with low residence times of particles in the “hot flame”, it is noticeable decomposition of HAp into C_3P/C_{4P} or CaO [51], this can be observed in figure 9 above. HAp loses many hydroxyl groups above 1300 °C and studies have revealed that at >1350 °C, the strength of HA drastically decreases [47] [30].

The higher the Argon gas flow the higher velocity and less the influence of heat over the particles so that larger Titanium particles do not melt and the less sever environment allows the HAp to reach the substrate more “untouched” and show higher crystallinities due to reduce the melting degree of the powder. The results with high Argon flow show that with a low ratio of H_2 it is suitable to spray.

3.2.4 APS H_2 Secondary Gas Flow parameters setting

Table 14-Analysis results for variation of H_2 gas flow levels

Parameters Program 1 Variation of H_2 Secondary Gas Flow					
Levels	1	2	3	4	5
Parameter Values (NLPM)	X	X_1	X_2	X_3	X_4
Crystallinity (%)	21,44	18,48	15,84	17,76	15,63
Adhesion (MPa)	19,67 ± 4,34	22,66 ± 5,32	27,88 ± 5,67	25,03 ± 3,43	18,76 ± 4,76
Thickness (µm)	175	120	150	185	220
Average roughness R_a (µm)	R_a = 9,81 R_t = 46,55 R_z = 45,24	R_a = 8,40 R_t = 53,72 R_z = 48,98	R_a = 10,73 R_t = 67,43 R_z = 48,98	R_a = 11,86 R_t = 61,48 R_z = 58,23	R_a = 11,89 R_t = 65,12 R_z = 50,13
Respective Image	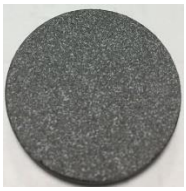	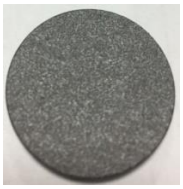	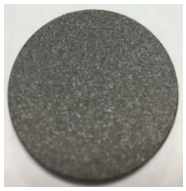		
Respective Image After G Type Acid vol. 65% treatment	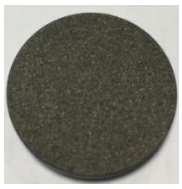		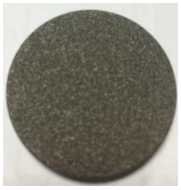	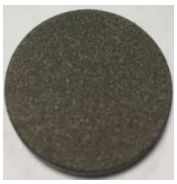	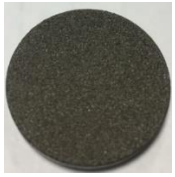

H_2 addition, in small quantities, to argon leads to increased plasma enthalpy and its temperature [42]. This increases the heat transfer rates from the plasma to the powder particles and promotes the melting of the powder particles. On figure 12 its clear that the higher the H_2 flow the higher the temperature achieved, since the CaO phase increases its peak accordingly. Results with low H_2 flow show that it is more suitable in terms of crystallinity. However, it also shows a trend of low thickness and a short value for R_t meaning a weak melting of Titanium particles and a capacity for only melting the smaller ones.

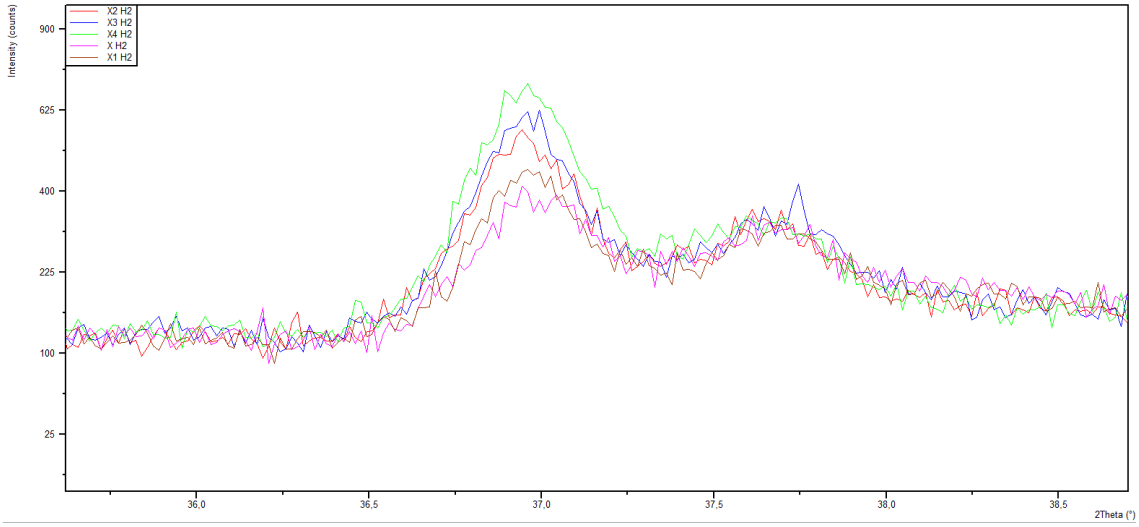

Figure 12-H_2 flow challenging influence on CaO phase peak

Based on the previous preliminary analysis, and taking in to account that, due to the presence of Titanium particles, most of the adhesion values were above that of the single HAp. After this assessment it was prioritized to improve the coating crystallinity since good values for adhesion strength were observed, and without a good crystallinity there was no logic in focusing first on improving the coating adhesion. Also each adhesion test is extremely expensive to perform in comparison to DRX. The choice of the lowest and highest levels for each parameter was based on the crystallinity values and trends during the parameters study.

3.3 Best levels range selection for further study

A range for each parameter was pre-selected according to values on the table 15.

Table 15-Pre-selected low and high level for each parameter range selected based on the preliminary study of program 1

Parameters	**Values**	
	Low Level (-)	**High Level (+)**
Power (Amps)	Z_{-1}	Z_1
Spray flame distance (mm)	R_{-2}	R_{-1}
Primary Gas Flow Rate (NLPM)	V_1	V_2
Secondary Gas Flow Rate (NLPM)	X	X_1

3.4 Screen test by full factorial with 2 levels

In order to tackle such a multi-response optimization problem, the present study is to find out the optimal setting of parameters of APS for production of the Titanium/HAp composite coating. Parameter selection for APS process with a mixture of Titanium and HAp on a stainless steel substrate was made by choosing the right combination of Power feed, Nozzle Distance, Gas flow, and type of gas used to achieve desired HAp phase crystallinity with maximum pull-out strength from the coating.

Following the preliminary study, the highest and lowest level for each parameter pre-selected on the machine was defined. Design of experiments was applied and several experiments were planned and performed according to a random order obtained by a specialized software for the matter, Statistica[3]. Four main factors were preliminarily identified to have a direct influence on the crystallinity of the coating: plasma power (A), nozzle distance to the target (B), primary gas flow of Argon(C) and secondary gas flow of H_2 (D), with two levels each. All experiments were done in replicate to access the variance of results. With this work, the objective is to identify the best combination of levels for the factors and achieve the highest value possible for the coatings crystallinity, since in overall the adhesion results were above the average HAp values. The "answer" or result values (Y) are crystallinity results for each experiment according to the factor levels.

3.4.1 Control of experimental data

Identification of transformation parameter (λ). All the data has to be analyzed in order to confirm the normality of data and homogeneity of variance. The objective is to obtain a normal distribution of the transformed data (after transformation) and a constant variance.

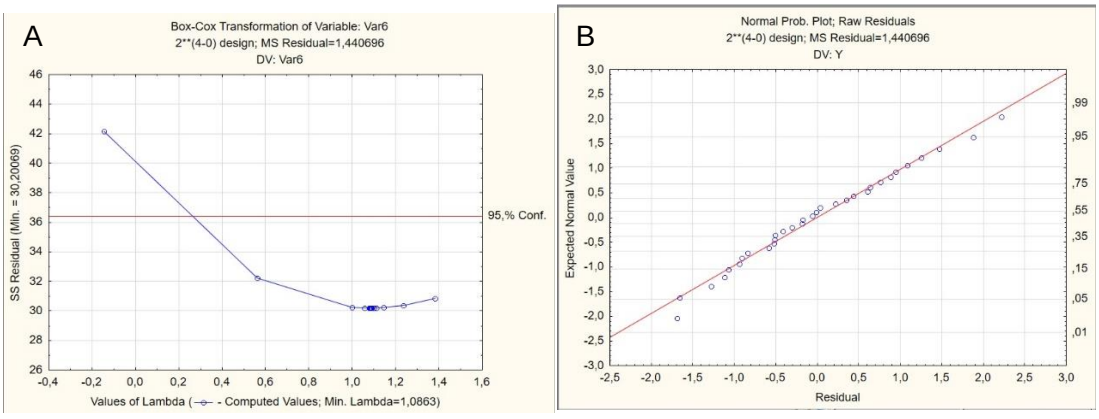

Figure 13- Box-Cox chart A and Normal distribution probability chart B for analyzing experimental data

[3] Table of random experiences generated by Statistica software and respective coating crystallinity results in Annex III.

Normally distributed data is needed to use a number of statistical analysis tools, such as analysis of variance (ANOVA). When data is not normally distributed, the cause for non-normality should be determined and appropriate remedial actions should be taken. Data transformation, and particularly the Box-Cox power transformation, is one of these remedial actions that may help to make data normal. However as can be seen from the left graph analysis, the value of λ = 1 is within the confidence interval has can be observed in figure 12 -A, so it is not necessary to transform the data to continue the study. The conditions of homogeneity of the variance and the normality of the model data are verified. If in the experience, there are genuine replicates and their time order it is known it is important to look at their plots to see if they might have some significant trending. Even with randomization a trend of this type will point towards some unaccounted for variable that, for this design, was part of the estimate of error. The Normal Distribution probability graph in figure 12-B shows that the residuals are arranged in a straight line (approximately), concluding that the Normality assumption of the residuals is satisfied.

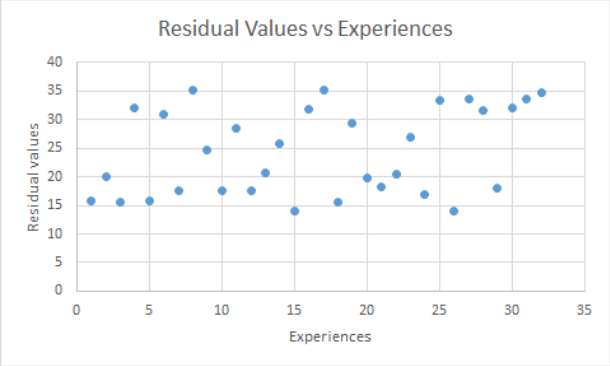

Figure 14-Dispersion chart of Residual values Vs Experiences runs

The chart of the residuals shown in figure 12, according to the random order by which the experiments were carried out shows a randomness and no observable trend in the way the points are arranged. Observing the data distribution, it is assumed that the assumption of constant variance is not violated. They are scattered around zero, from which it is inferred that the errors are distributed with zero mean.

3.4.2 ANOVA

An ANOVA table was created, where (1) is referring to factor A, (2) is factor B, (3) factor C and (4) factor D. And their interactions 1 by 2 is equivalent to AB, 1 by 3 equivalent to AC and so on.

Factor	SS	df	MS	F	p
ANOVA; Var.:Var6; R-sqr=,98296; Adj:,97485 (Spreadsheet5) 2**(4-0) design; MS Residual=1,440696 DV: Var6					
(1)Var2	25,347	1	25,347	17,594	0,000408
(2)Var3	18,850	1	18,850	13,084	0,001617
(3)Var4	1539,848	1	1539,848	1068,822	0,000000
(4)Var5	98,772	1	98,772	68,558	0,000000
1 by 2	0,088	1	0,088	0,061	0,806980
1 by 3	3,768	1	3,768	2,615	0,120777
1 by 4	31,166	1	31,166	21,632	0,000137
2 by 3	0,053	1	0,053	0,037	0,850003
2 by 4	9,702	1	9,702	6,734	0,016898
3 by 4	17,701	1	17,701	12,287	0,002106
Error	30,255	21	1,441		
Total SS	1775,548	31			

Figure 15-Statistica generated ANOVA

Not all interactions revealed to become significant. Only the ones presented in red lettering. To better visualize each factor and interaction significance to crystallinity values a Pareto Chart was created and showed below.

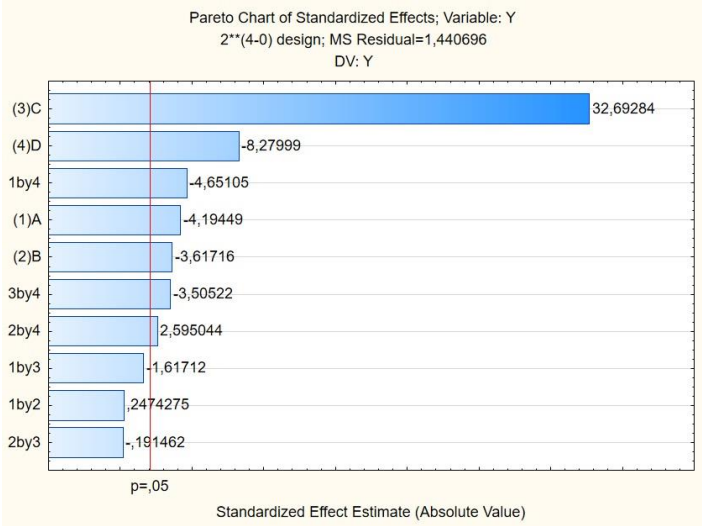

Figure 16-Statistica software generated Pareto chart

This leads to a new ANOVA where all the interactions without influence are removed and the table is recalculated has shown in figure 16 bellow. The F-value in the ANOVA table indicates the extent of the effect of each factor on the crystallinity, the higher the F-value the greater the effect. Primary Gas Flow (Argon) showed the greater significance in terms of influencing crystallinity.

	ANOVA; Var.:Var6; R-sqr=,98076; Adj:,97515 (Spreadsheet25 in EXCEL DADOS STATISCT ALEATORIO) 2**(4-0) design; MS Residual=1,423465 DV: Var6				
Factor	SS	df	MS	F	p
(1)Var2	25,347	1	25,347	17,807	0,000302
(2)Var3	18,850	1	18,850	13,242	0,001305
(3)Var4	1539,848	1	1539,848	1081,760	0,000000
(4)Var5	98,772	1	98,772	69,388	0,000000
1 by 4	31,166	1	31,166	21,894	0,000094
2 by 4	9,702	1	9,702	6,816	0,015329
3 by 4	17,701	1	17,701	12,435	0,001726
Error	34,163	24	1,423		
Total SS	1775,548	31			

Figure 17-Statistica generated ANOVA after removal of low significance factors and interactions

3.4.3 Best Levels selection

For crystallinity values the higher the better. Factor levels and interactions with higher absolute value are sought[4].

There is no conflict between the different interactions BD and CD in assigning the best level in factors B, C, D. for the majority of factors and the interactions have the same levels when assumed for “highest value”. Therefore, the best levels are B-, C+, D-. However, there is conflict for factor A; the best level of A depends on the resolution of the conflict between the interactions AD with the factor A. The selection criteria chosen is based on the perception of significant interaction, obtained by the contour surfaces. When analyzing the figure 24 below its perceptible that A+ is the best from both levels, also looking at the Pareto chart from figure 15 the interaction AD has more significance so the best levels for A is + and not -, since A+ is completely in the >26 area (red), that can be seen in figure 24 below. Even though that both levels are really close in terms of results between the 2 levels. By looking at table 12 from the preliminary study at Z1 A better result was obtained for adhesion strength so for a future optimization of the coating this also should be taken into account for choosing level A+.

[4] Marginal Means values for each factor and significant integrations are in Annex IV.

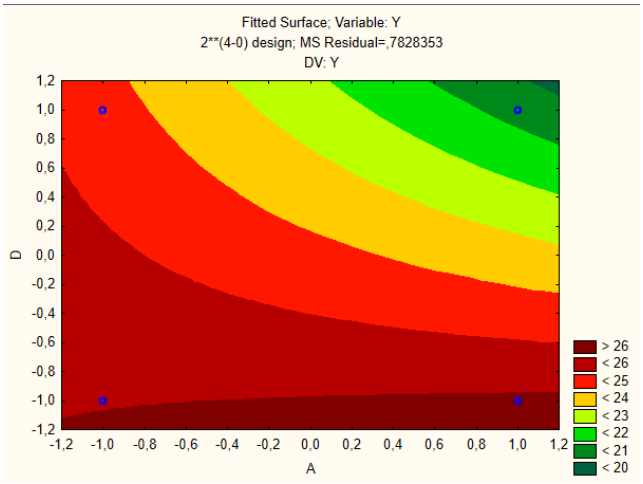

Figure 18-Contour surface graph generated by Statistica for interaction AD

Table 16- Best levels achieved

Best levels (α=5%)
A^+
B^-
C^+
D^-
A^+D^-
B^-D^-
C^+D^-

The higher this perception, the greater the contribution of this interaction to minimize the response. In support of this criteria, AD has greater contribution (ρ) than the remaining interactions. As only interaction AD is significant, or more significant than the rest, the best level of factor A is there for being A +.

Table 17-Best parameter levels achieved for crystallinity values

Best parameter levels achieved for crystallinity values				
Parameter	**Plasma power (A)**	**Plasma Nozzle Distance (B)**	**Primary Gas Flow Argon (C)**	**Secondary Gas Flow H_2 (D)**
Level	+	-	+	-
Value	Z_1	R_{-1}	V_2	X

3.4.4 Confirmation Experience

Has $F_{5\%,1,24}$=4,26 all factors A, B, C, D and interaction AD, BD and CD affect signicantly answer Y, according to figure 16. Values obtained for these affects can be used to calculated the residues between values observed and vales expected for each experience.

$$\hat{Y} = \bar{y} - (Effect\ A)/2 - (Effect\ B)/2 + (Effect\ C)/2 - (Effect\ D)/2 + (Effect\ AD)/2 + (Effect\ BD)/2 + (Effect\ CD)/2 = 24{,}29 - (-1{,}78/2) - (-1{,}53/2) + (13{,}87/2) - (-3{,}51/2) + (1{,}97/2) + (1{,}10/2) + (1{,}48/2) = 36{,}91\%$$

$F_{\alpha=5\%;1;4}$= 4,26 ; C=1 since only one replica was performed & ne = $\frac{32}{1+7} = 4$

IC= $\bar{y} \pm \sqrt{F\alpha = 5\%; 1; 24 * MSErro * \left(\frac{1}{ne} + \frac{1}{c}\right)} = [34{,}16; 39{,}66]$

The confirmation experience was performed using the same best levels has shown at table 17. The coating reached a 90 µm thickness using also 5 passes of the plasma gun from the original program. A roughness R_a of 10,03 µm was achieved with a R_t of 53,63 µm. The coating crystallinity had a value 34,31% using the best levels[5], its value fits inside the predicted confidence range, therefore it is a valid and well executed planning, leading to satisfactory results. Also the adhesion strength of the coating showed a value of 18,89 ± 3,76 MPa, meaning an acceptable range despite its standard deviation presenting a higher value then former testing before.

[5] A visual comparing image of the coating on a stainless steel spinal screw test sample vs single HAp coated screw in Annex V

CHApter 5

5

Conclusions and future perspectives

This dissertation compiles the work to start exploring a low cost easily producible composite coating as a substitute for the existing medical implant spinal screws' coatings using single layers of HAp. The final goal of the dissertation was to obtain a fully functional coating that would be improved in terms of properties and would respect the current standards used in the industry for medical graded coatings. To fulfil this objective several different tasks were set:

1. To manufacture a reliable composite mixture;
2. To test the viability of the composite turning it into a hard coating trough APS system and pre-selected program;
3. Determine the coating properties according to already used industry standards;
4. Access the best combination of the APS parameter levels to achieve high crystallinity.

The first task was accomplished using a Turbula Mixer equipment to mix current Titanium and HAp batches used at CERAMED S.A. facilities. The mixture proved to be difficult to process and only one formula (60%Titanium40%HAp mass ratio during J3h at L RPM) with a reduced standard deviation was reliable enough to carry on. After this first task it was of the most importance to ensure that the ratio and dispersion would be the same in the powder and in the coating, produced by APS.

The preliminary study used with program 1 parameters allowed to confirm and comprehend the direct influence of each parameter in key coating properties such as thickness, adhesion strength, crystallinity and surface roughness.

Plasma power showed a big impact on the adhesion strength due to its capability in changing "flame" temperature and melt bigger particles has showed with rising R_t values, specifically Titanium ones. Only the medium range between Z_{-1}-Z_1 proved usable in

the composite. Power given also presented a big direct effect on the crystallinity values where the lowest were the best and the highest the worst.

The Plasma Spray Gun Distance showed no significant improvement on the crystallinity; even though the closer the better. In terms of adhesion strength also the medium ranges proved more suitable then the extremes, since at close proximity the irremediably damaged. At a greater distance a substantial decrease in the thickness of the coating was observed, also suggesting dispersion of the particles and of course less efficacy of the coating process.

The Primary Gas Flow with Argon showed direct influence on the particles speed due to pressure forces projected by the "flame". With the increasing of gas flow, particles reached higher speed meaning that HAp particles would not be so affected by thermal energy, increasing crystallinity rates. The same way with Titanium particles, however these have higher melting points so a more and more would bounce off increasingly according decreasing severely its thickness.

Secondary Gas Flow showed a major contribution for temperature levels and a relation between the primary gas and secondary was also observable crossing the results between the two. The higher the H_2 the less visually white appeared on the samples and accordingly the lower the crystallinity levels, compatible with an increase in the HAp decomposition.

With the Screening test it was possible to confirm that the preliminary conclusions about the more suitable ranges for the composite coating crystallinity using four primary APS system parameters. With a low variability experiment is safe to assume that this study constituted the first steps for a complete optimization of Ti/HAp APS coatings using a 3 level factorial. The predicted confidence range given by the confirmation experience showed that the composite crystallinity is close to that of the standards (> 45%). Also the best levels confirmation experienced presented a value still above the minimum requirement for HAp, even dough under the minimum for the Titanium requirement. In a future study best levels achieved would become the middle value for a shorter range of the parameters levels. The ultimate objective is to try to make a coating above the imperative >45% crystallinity and with a strong adhesion strength, however both objectives are hard to come hand in hand, so independent optimization studies will be required.

In the future some complementary proceedings can be tested for increasing the crystallinity value. Such has like decreasing the air cooling flow to try to increase recrystallization, which has shown to work before on single layer of HAp. Also post-spray heat treatment has proved to work before effectively restoring the structural integrity of HAp by transforming non-HAp phases into HAp [44], even though this might considerably increase the production cost.

If achieved the composite could represent a good alternative to current HAp as in terms of performance according to standards. Also in terms of manufacture cost, since for a start, 60% of the composite layer material mass would be replaced by Titanium much cheaper commercially [15], also if the improvement is achieved it would represent a simple single step process, unlike double and graded coating.

Even though that with an optimization a crystallinity level much higher than 45% will be really hard to reach without compromising the adhesion strength and the melting of Titanium particles a plausible working coating might be reached.

CHApter 6

6

I-Annex

APS functioning and parameter description

Plasma Spray

Plasma Spray surface coating method is a technology where powder particles are injected into Plasma and after projected into a surface creating a hard coating. Thereby particles start to melt on the surface all the way to the nucleus depending on the conditions applied (temperatures can rise up to 10000 K), and are accelerated towards a "defined target" in order to create new surfaces on a variety of substrates. An Atmospheric Plasma system is composed by a cathode and a nozzle shaped anode both consisting of two water-cooled electrodes, between these electrodes gas carriers formed by an inert gas, are forced through it in a continuous flow and an electric arc charge (high energy discharge) is applied promoting dissociation and ionization of plasma forming gases. The charge can be AC or DC allowing for better levels of noise and signal fluctuation. With a continuous flow of gas and high voltage discharge the plasma is "created" and contained inside the chamber where the two electrodes are, only escaping trough the nozzle of the anode.

Process Parameters

The quality of plasma coatings is controlled by as many as 50 process parameters [42] of witch these only twelve parameters are considered primary since they can be directly controlled by the user [51] . Because of various economic reasons and time requirements it is not possible to control all possible parameter variations. Based on information from the literature and knowhow it is possible to identify the more relevant parameters to study and challenge. Primary APS parameters used for this study are found on table 18 below.

Table 18- Primary APS parameters used for this study

Primary parameters	Study
Powder Particle Morphology	Fixed
Plasma Flame Temperature	Impossible to access no system available
Powder Particle Composition	Fixed -60% supplier 1 Titanium Powder and 40% supplier 3 HAp powder
Powder Injection Angle	Fixed- 90º
Flame Plasma Forming Gas	Challenged- Argon
Secondary Gas	Challenged H_2
Forming Gas Flow Rate	Challenged
Current	Challenged
Substrate Temperature	Fixed- Ambient temperature 25ºC
Power	Challenged
Carrier Gas	Fixed- Argon
Carrier Gas Flow Rate	Fixed T NPLM
Coating Thickness	Dependent on the process parameters challenged
Spray Distance	Challenged
Substrate Material	Fixed- Steel Type 316
Substrate Surface Properties	Fixed- Roughness between 3-7 μm
N º of Passes of Plasma Gun	5
Powder Feeder Rate	W% Rotation Q% Vibration

Plasma Power

The principle of this method of generating plasma is by the formation of an electric current in a gas between the anode and the cathode accelerating charge carriers in an electric field with subsequent energy transfer by collision. The power supplied was also found to cause an increase both in the temperature and the velocity of the plasma flame [42].

A low level in power may result in high porosity of the coating [52], due to many particles becoming un-melted or partially melted so once they hit the substrate their solidification happens to fast and the interaction with other melted cores low, leaving many gaps between particles. On the opposite too much power may lead to high residual stresses, in which both factors gave negative effects on the micro hardness.

Power is proportional to the voltage that is associated to the current.

Distance of the nozzle

The Plasma Spray "flame" is canalized trough a nozzle and is supported by a programmable robotic arm. During the process it performs several movements in order to cover and spray the surface intended according to its shape and size. These movements are repeated through several cycles so that the target surface material does not overheat and become damaged, allowing to cool it down in between with the help of air pressurizers. The more the thickness desired the more cycles each one presenting a new top layer. A shorter distance between the nozzle and the substrate the more thermal energy is absorbed by the coating is maintained at a higher temperature for longer, allowing for recrystallization to occur.

Plasma Forming Gases

Argon is a noble and inert gas probably the most used primary plasma gas as it is inert, cheap and relatively simple to form a plasma since its electrons have a high energy levels, meaning an outer shell of electrons are easy to be separated also tends to be less aggressive towards electrode and nozzle hardware. Most plasmas are started up using pure argon and then used with a secondary plasma gas (Hydrogen, Helium and Nitrogen) to increase its energy.

As a secondary gas Nitrogen and Hydrogen are diatomic gases because of the energy released in the dissociation of molecules these plasmas have higher energy contents for a given temperature than the atomic gases of argon and helium being monoatomic. They are used as secondary gases and addition, in small quantities, to argon leads to increased plasma enthalpy [42]

Nitrogen is a cheap gas and tends to be inert however has the potential to react with the sprayed materials like Titanium [54].

Hydrogen is mainly used as a secondary gas, it dramatically effects heat transfer properties and acts as anti-oxidant.

Powder Feed Rate

The rate at which powder is fed into the plasma flame has two main effects it affects the quantity of particles available at the and therefor the thickness of the coating [42], never the less its influence is small. The feeding rate when too high appears to have a harmful effect on the efficiency of the process, too many on the flame and it will lead to a competition for thermal energy although its influence is small, consequentially larger fractions of unmelted or semi-melted particles will be projected onto the substrate creating a not so strong coating layer [52]. Agitation and Rotation of the stock feeder was discarded has a parameter to include on this study, since both in size and density HAp and Titanium had identical values and their influence is resumed the coating thickness and roughness.

Powder Carrier Gas

The carrier gas normally Argon is used to carry the particles through a tube system its influence is pretty low and controllable. Depending on the flow it presents changes on the amount of particles sent onto the “gun” and thereby the thickness of the coating and its roughness.

Robotic Arm

The Plasma Spray Gun Nozzle is attached to a robotic arm, this equipment ultimately controls the nozzle distance, movement speed, time and number of times performed every passing cycle through the process.

II-Annex

DOE experimental description

A DOE methodology implementation allows to achieve a good knowledge of parameters for certain study cases like the APS system. These parameters are so called factors and they influence, or not, a certain process. This method allows for an identification of the most suitable levels for the factors, accordingly with the objective intended, in the case of this study, the highest crystallinity possible.

For this to be possible a good control of the process is required, and there for a low variation of results is essential. In order to ensure a homogeneity of variance of the results and the normality of the data, Box Cox Method was chosen. In this method data was transformed and an analysis of variability was performed. The best value for a minimum residual variability is when λ is at lowest point.

In a two level DOE, both levels are designated by high and low, respectively + and –, or 1 and -1. It is up the investigator to decide which are the suitable levels for each factor. In this study a preliminary design was performed in order to comprehend each factor individual behavior and influence on key properties (crystallinity, adhesion strength, thickness and roughness), and also factors interactions influences. Each change in the result caused by a level variation is considered an “effect”.

In this case using a full factorial for four primary parameters of the APS system a different set of objectives was pursued. Experimenting with the different four factors (Plasma Power, Nozzle Distance, Primary Gas Flow and Secondary Gas Flow), for maximum efficiency to determine both the factor and their interactions effects and significance. Also the experimental associated error involved was determined.

Following the factors assessment in terms of influence in order to obtain a high crystallinity a best combination of factors was determined using a combination between the two best range of levels previously accessed on preliminary study. However, this best combination is punctual, so there is a need to ensure a model that that allows the prediction of results. By using Chebyshev orthogonal polynomials it was possible to determine such a range since, the studied factors only have two levels meaning that their variations will only have a linear component. Where the regression coefficients are equal to the half of factors and interactions effects values.

Using an empirical model, a set of predicted values was calculated for the best combination of factor levels. this range allowed to establish a base for a future optimization such as the 3 level factorial.

III-Annex

Design Off Experiments random order

RUN	REPLICA	A	B	C	D	(Y)%
28	2	+	+	-	+	15,77
18	2	+	-	-	-	20,07
12	1	+	+	-	+	15,57
13	1	-	-	+	+	32,02
19	2	-	+	-	-	15,76
29	2	-	-	+	+	30,95
25	2	-	-	-	+	17,59
6	1	+	-	+	-	35,14
16	1	+	+	+	+	24,61
4	1	+	+	-	-	17,57
30	2	+	-	+	+	28,59
27	2	-	+	-	+	17,59
1	1	-	-	-	-	20,73
32	2	+	+	+	+	25,78
10	1	+	-	-	+	14,02
24	2	+	+	+	-	31,76
21	2	-	-	+	-	35,21
3	1	-	+	-	-	15,48
31	2	-	+	+	+	29,36
17	2	-	-	-	-	19,86
11	1	-	+	-	+	18,28
2	1	+	-	-	-	20,47
14	1	+	-	+	+	26,93
20	2	+	+	-	-	17,00
8	1	+	+	+	-	33,43
26	2	+	-	-	+	13,99
22	2	+	-	+	-	33,72
15	1	-	+	+	+	31,58
9	1	-	-	-	+	17,92
23	2	-	+	+	-	32,06
5	1	-	-	+	-	33,73
7	1	-	+	+	-	34,78

IV-Annex

Marginal Means

For crystallinity values the higher the better. Factor levels and interactions with higher means absolute value are sought.

Marginal Means (Unweighted); variable: Y (Spreadsheet5 in dadoss)
Design: 2**(4-0) design
NOTE: Std.Errs. for means computed from MS Error=1,440696

A	Means	Pooled Std.Dev.	Overall Std.Dev.	N	Std.Err. for Mean	-95,% Cnf.Limt	+95,% Cnf.Limt
-1,	25,18125	1,033272	7,738104	16	0,300073	24,55721	25,80529
1,	23,40125	0,768749	7,536697	16	0,300073	22,77721	24,02529

Figure 19-Marginal Means generated by Statistica for Factor A

Best level Factor A - A- = 25,18125

Marginal Means (Unweighted); variable: Y (Spreadsheet5 in dadoss)
Design: 2**(4-0) design
NOTE: Std.Errs. for means computed from MS Error=1,440696

B	Means	Pooled Std.Dev.	Overall Std.Dev.	N	Std.Err. for Mean	-95,% Cnf.Limt	+95,% Cnf.Limt
-1,	25,05875	0,755563	7,732395	16	0,300073	24,43471	25,68279
1,	23,52375	1,042953	7,571214	16	0,300073	22,89971	24,14779

Figure 20-Marginal Means generated by Statistica for factor B

Best level Factor B - B- = 25,05875

Marginal Means (Unweighted); variable: Y (Spreadsheet5 in dadoss)
Design: 2**(4-0) design
NOTE: Std.Errs. for means computed from MS Error=1,440696

C	Means	Pooled Std.Dev.	Overall Std.Dev.	N	Std.Err. for Mean	-95,% Cnf.Limt	+95,% Cnf.Limt
-1,	17,35438	0,348757	2,166429	16	0,300073	16,73034	17,97841
1,	31,22813	1,239756	3,319631	16	0,300073	30,60409	31,85216

Figure 21-Marginal Means generated by Statistica for factor C

Best level Factor C - C^+ = 31,22813

Marginal Means (Unweighted); variable: Y (Spreadsheet5 in dadoss)
Design: 2**(4-0) design
NOTE: Std.Errs. for means computed from MS Error=1,440696

D	Means	Pooled Std.Dev.	Overall Std.Dev.	N	Std.Err. for Mean	-95,% Cnf.Limt	+95,% Cnf.Limt
-1,	26,04813	0,991032	8,118636	16	0,300073	25,42409	26,67216
1,	22,53438	0,822485	6,772950	16	0,300073	21,91034	23,15841

Figure 22-Marginal Means generated by Statistica for factor D

Best level Factor D - D^- = 26,04813

Marginal Means (Unweighted); variable: Y (Spreadsheet5 in dadoss)
Design: 2**(4-0) design
NOTE: Std.Errs. for means computed from MS Error=1,440696

A	D	Means	Pooled Std.Dev.	Overall Std.Dev.	N	Std.Err. for Mean	-95,% Cnf.Limt	+95,% Cnf.Limt
-1,	-1,	25,95125	1,141496	8,777980	8	0,424367	25,06873	26,83377
-1,	1,	24,41125	0,912298	7,064164	8	0,424367	23,52873	25,29377
1,	-1,	26,14500	0,813188	8,010377	8	0,424367	25,26248	27,02752
1,	1,	20,65750	0,721578	6,351753	8	0,424367	19,77498	21,54002

Figure 23-Marginal Means generated by Statistica for Interaction AD

Best level Interaction AD – A^+ + D^- = 26,14500

Marginal Means (Unweighted); variable: Y (Spreadsheet5 in dadoss)
Design: 2**(4-0) design
NOTE: Std.Errs. for means computed from MS Error=1,440696

C	D	Means	Pooled Std.Dev.	Overall Std.Dev.	N	Std.Err. for Mean	-95,% Cnf.Limt	+95,% Cnf.Limt
-1,	-1,	18,36750	0,406233	2,163686	8	0,424367	17,48498	19,25002
-1,	1,	16,34125	0,279710	1,740595	8	0,424367	15,45873	17,22377
1,	-1,	33,72875	1,341366	1,311536	8	0,424367	32,84623	34,61127
1,	1,	28,72750	1,129037	2,757026	8	0,424367	27,84498	29,61002

Figure 24-Marginal Means generated by Statistica for interaction CD

Best level Interaction BD – B^- + D^- = 27,36625

Marginal Means (Unweighted); variable: Y (Spreadsheet5 in dadoss)
Design: 2**(4-0) design
NOTE: Std.Errs. for means computed from MS Error=1,440696

B	D	Means	Pooled Std.Dev.	Overall Std.Dev.	N	Std.Err. for Mean	-95,% Cnf.Limt	+95,% Cnf.Limt
-1,	-1,	27,36625	0,800289	7,596994	8	0,424367	26,48373	28,24877
-1,	1,	22,75125	0,708017	7,631288	8	0,424367	21,86873	23,63377
1,	-1,	24,73000	1,150576	8,919355	8	0,424367	23,84748	25,61252
1,	1,	22,31750	0,922862	6,320989	8	0,424367	21,43498	23,20002

Figure 25-Marginal Means generated by Statistica for interaction BD

Best level Interaction CD – C^{+} + D^{-} = 33,72875

V-Annex

Visual comparing image of the coating on a stainless steel spinal screw test sample vs single HAp coated screw

Image 1 - Visual looks comparison between HAp coated spinal screw thread (left) vs 60%Ti/40%Hap composite coated spinal screw thread using best levels achieved (right)

References

[1] Lesic A, Zagorac S, Bumbasirevic V and Bumbasirevic M 2012 The development of internal fixation: Historical overview *Acta Chir. Iugosl.* **59** 9–13

[2] Requirements M Internal Fixation Under Msf Settings - Minimal Requirements and Limitations – 1–7

[3] Baxter R, Hastings N, Law a. and Glass E J . 2008 [No Title] *Anim. Genet.* **39** 561–3

[4] Kaur K 2013 Stainless Steel and Titanium in Surgical Implants *Stainl. Steel Titan. Surg. Implant.* 1–3

[5] Van Manen M D, Nace J and Mont M A 2012 Management of primary knee osteoarthritis and indications for total knee arthroplasty for general practitioners *J Am Osteopat. Assoc* **112** 709–15

[6] Brown R N, Sexton B E, Gabriel Chu T M, Katona T R, Stewart K T, Kyung H M and Liu S S Y 2014 Comparison of stainless steel and titanium alloy orthodontic miniscrew implants: A mechanical and histologic analysis *Am. J. Orthod. Dentofac. Orthop.* **145** 496–504

[7] Oldani C and Dominguez A 2012 Titanium as a Biomaterial for Implants *Recent Adv. Arthroplast.*

[8] Erli H J, Marx R, Paar O, Niethard F U, Weber M and Wirtz D C 2003 Surface pretreatments for medical application of adhesion *Biomed. Eng. Online* **2** 1–18

[9] Marx R, Qunaibi M, Wirtz D C, Niethard F U and Mumme T 2005 Surface pretreatment for prolonged survival of cemented tibial prosthesis components: Full- vs. surface-cementation technique *Biomed. Eng. Online* **4** 1–9

[10] Kleppel D, Stirton J, Liu J and Ebraheim N A 2017 Antibiotic bone cement's effect on infection rates in primary and revision total knee arthroplasties *World J. Orthop.* **8** 946–55

[11] Abu-Amer Y, Darwech I and Clohisy J C 2007 Aseptic loosening of total joint replacements: Mechanisms underlying osteolysis and potential therapies *Arthritis Res. Ther.* **9** 1–7

[12] Galante J and Rostoker W 1973 Fiber metal composites in the fixation of skeletal prosthesis *J. Biomed. Mater. Res.* **7** 43–61

[13] Chang Y S, Oka M, Kobayashi M, Gu H O, Li Z L, Nakamura T and Ikada Y 1996 Significance of interstitial bone ingrowth under load-bearing conditions: A comparison between solid and porous implant materials *Biomaterials* **17** 1141–8

[14] Abe L, Nishimura I and Izumisawa Y 2008 Mechanical and histological evaluation of improved grit-blast implant in dogs: pilot study *J Vet Med Sci* **70** 1191–8

[15] Zhou X 2012 Hydroxyapatite/Titanium Composite Coating For Biomedical Application

[16] Vladescu A, Birlik I, Braic V, Toparli M, Celik E and Ak Azem F 2014 Enhancement of the mechanical properties of hydroxyapatite by SiC addition *J. Mech. Behav. Biomed. Mater.* **40** 362–8

[17] Geesink R G T, Groot K De and Klein C P A T 1987 Chemical Implant Fixation Using Hydroxyl-Apatite Coatings. *Clin. Orthop. Relat. Res.* 147–70

[18] Sopyan I, Mel M, Ramesh S and Khalid K A 2007 Porous hydroxyapatite for

artificial bone applications *Sci. Technol. Adv. Mater.* **8** 116–23
[19] Prakasam M, Locs J, Salma-Ancane K, Loca D, Largeteau A and Berzina-Cimdina L 2015 Fabrication, properties and applications of dense hydroxyapatite: A review *J. Funct. Biomater.* **6** 1099–140
[20] Chandramohan D and Marimuthu K 2010 Contribution of Biomaterials to Orthopaedics as Bone Implants -A Review *Int. J. Mater. Sci.* **5** 973–4589
[21] Tozzi G, De Mori A, Oliveira A and Roldo M 2016 Composite hydrogels for bone regeneration *Materials (Basel).* **9** 1–24
[22] Søballe K 1993 Hydroxyapatite ceramic coating for bone implant fixation: Mechanical and histological studies in dogs *Acta Orthop.* **64** 1–58
[23] Barrère F, van Blitterswijk C A and de Groot K 2006 Bone regeneration: Molecular and cellular interactions with calcium phosphate ceramics *Int. J. Nanomedicine* **1** 317–32
[24] Yip C S, Khor K A, Loh N L and Cheang P 1997 Thermal spraying of Ti□6Al□4V/hydroxyapatite composites coatings: powder processing and post-spray treatment *J. Mater. Process. Technol.* **65** 73–9
[25] Tsui Y C, Doyle C and Clyne T W 1998 Plasma sprayed hydroxyapatite coatings on titanium substrates Part 1: Mechanical properties and residual stress levels *Biomaterials* **19** 2015–29
[26] Mohseni E, Zalnezhad E and Bushroa A R 2014 Comparative investigation on the adhesion of hydroxyapatite coating on Ti-6Al-4V implant: A review paper *Int. J. Adhes. Adhes.* **48** 238–57
[27] Zheng X, Huang M and Ding C 2000 Bond strength of plasma-sprayed hydroxyapatite/Ti composite coatings *Biomaterials* **21** 841–9
[28] Ong J L, Carnes D L and Bessho K 2004 Evaluation of titanium plasma-sprayed and plasma-sprayed hydroxyapatite implants in vivo *Biomaterials* **25** 4601–6
[29] Chun-Cheng C, Tsui-Hsien H, Chia-Tze K and Shinn-Jyh D Characterization of functionally graded hydroxyapatite/titanium composite coatings plasma-sprayed on Ti alloys *J. Biomed. Mater. Res. Part B Appl. Biomater.* **78B** 146–52
[30] Lu Y P, Li M Sen, Li S T, Wang Z G and Zhu R F 2004 Plasma-sprayed hydroxyapatite+titania composite bond coat for hydroxyapatite coating on titanium substrate *Biomaterials*
[31] Rakngarm A and Mutoh Y 2009 Characterization and fatigue damage of plasma sprayed HAp top coat with Ti and HAp/Ti bond coat layers on commercially pure titanium substrate *J. Mech. Behav. Biomed. Mater.* **2** 444–53
[32] Literature C 1989 Current literature 213 1989–90
[33] Moroni A, Faldini C, Rocca M, Stea S and Giannini S 2002 Improvement of the bone-screw interface strength with hydroxyapatite-coated and titanium-coated AO/ASIF cortical screws *J. Orthop. Trauma* **16** 257–63
[34] Martinez-carranza N, Berg H E, Lagerstedt A, Nurmi-sandh H, Schupbach P and Ryd L 2014 Fixation of a double-coated titanium-hydroxyapatite focal knee resurfacing implant A 12-month study in sheep *Osteoarthr. Cartil.* **22** 836–44
[35] Xu J, Xie Z, Zhao J, Gao Y, Zhao H, Peng L and Qu Y 2016 Results of a hydroxyapatite-coated femoral stem (Corail) in Chinese: a minimum 10-year follow-up *Springerplus* **5**
[36] Hetherington V, E. Lord C and A. Brown S 1995 Mechanical and histological fixation of hydroxylapatite-coated pyrolytic carbon and titanium alloy implants: A report of short-term results *J. Appl. Biomater.* **6** 243–8
[37] Vilardell A M, Cinca N, Concustell A, Dosta S, Cano I G and Guilemany J M 2015 Cold spray as an emerging technology for biocompatible and antibacterial coatings : state of art Cold spray as an emerging technology for biocompatible and antibacterial coatings : state of art *J. Mater. Sci.*
[38] Muhammad M M, Jalar A, Shamsudin R and Isa M C 2014 Effect of plasma spray

parameters on porosity of fly ash deposited coatings *AIP Conf. Proc.* **1614**
[39] Bauman I, Ćurić D and Boban M 2008 Mixing of solids in different mixing devices *Sadhana - Acad. Proc. Eng. Sci.* **33** 721–31
[40] Mayer-Laigle C, Gatumel C and Berthiaux H 2015 Mixing dynamics for easy flowing powders in a lab scale Turbula® mixer *Chem. Eng. Res. Des.* **95** 248–61
[41] Shackley M S 2018 X-Ray Fluorescence Spectrometry (XRF)
[42] Levingstone T 208AD Optimisation of Plasma Sprayed Hydroxyapatite Coatings *Thesis* 256
[43] Arifin A, Bakar A, Muhamad N, Syarif J and Ikram M 2014 Material processing of hydroxyapatite and titanium alloy (HA / Ti) composite as implant materials using powder metallurgy : A review Material processing of hydroxyapatite and titanium alloy (HA / Ti) composite as implant materials using powder metallurgy : A review *J. Mater.* **55** 165–75
[44] Chu C, Xue X, Zhu J and Yin Z 2006 Fabrication and characterization of titanium-matrix composite with 20 vol% hydroxyapatite for use as heavy load-bearing hard tissue replacement *J. Mater. Sci. Mater. Med.* **17** 245–51
[45] Chien C S, Han T J, Hong T F, Kuo T Y and Liao T Y 2009 Effects of Different Hydroxyapatite Binders on Morphology, Ca/P Ratio and Hardness of Nd-YAG Laser Clad Coatings *Mater. Trans.* **50** 2852–7
[46] Lu Y, Li M, Li S, Wang Z and Zhu R 2004 Plasma-sprayed hydroxyapatite + titania composite bond coat for hydroxyapatite coating on titanium substrate **25** 4393–403
[47] Arifin A, Sulong A B, Muhamad N, Syarif J and Ramli M I 2014 Material processing of hydroxyapatite and titanium alloy (HA/Ti) composite as implant materials using powder metallurgy: A review *Mater. Des.* **55**
[48] Mallik A K 2016 Preparation of HAp powder for Plasma Spray coating on SS 316 L
[49] Lucas M and Machado P 2018 hydroxyapatite-titanium oxide ceramic coating applied to Ti-6Al-4V alloys by plasma thermal spraying **21** 11–4
[50] Núñez D, Elgueta E, Varaprasad K and Oyarzún P 2018 Hydroxyapatite Nanocrystals Synthesized from Calcium rich Bio-wastes *Mater. Lett.*
[51] Heimann R B *Plasma- Spray Coating*
[52] Forghani S M, Ghazali M J, Muchtar A, Daud A R, Yusoff N H N and Azhari C H 2013 Effects of plasma spray parameters on TiO 2 -coated mild steel using design of experiment (DoE) approach *Ceram. Int.* **39** 3121–7
[53] Khor K A, Yip C S and Cheang P 1997 Ti-6Al-4V/hydroxyapatite composite coatings prepared by thermal spray techniques *J. Therm. Spray Technol.* **6** 109–15
[54] Guipont V, Molins R, Jeandin M, Barbezat G, Guipont V, Molins R, Jeandin M and Ti-al-v G B P 2002 Plasma-sprayed Ti-6Al-4V coatings in a reactive nitrogen atmosphere up to 250 kPa To cite this version : HAL Id : hal-01480135